

Phenomenological Studies on Melt-Structure-Water Interactions (MSWI) during Severe Accidents

B. R. Sehgal
Z. L. Yang
H. O. Haraldsson
R. R. Nourgaliev
M. Konovalikhin
D. Paladino
A. A. Gubaidullin
G. Kolb
A. Theerthan

May 2000

Phenomenological Studies on Melt-Structure-Water Interactions (MSWI) during Severe Accidents

B. R. Sehgal
Z. L. Yang
H. O. Haraldsson
R. R. Nourgaliev
M. Konovalikhin
D. Paladino
A. A. Gubaidullin
G. Kolb
A. Theerthan

Division of Nuclear Power Safety
Royal Institute of Technology
SE-100 44 Stockholm
Sweden

May 2000

SKI Project Number 99080

This report concerns a study which has been conducted for the Swedish Nuclear Power Inspectorate (SKI). The conclusions and viewpoints presented in the report are those of the authors and do not necessarily coincide with those of the SKI.

**PHENOMENOLOGICAL STUDIES ON
MELT-STRUCTURE-WATER INTERACTIONS
(MSWI) DURING SEVERE ACCIDENTS**

B.R. Sehgal, Z.L. Yang, H.O. Haraldsson, R.R. Nourgaliev
M. Konovalikhin, D. Paladino, A.A. Gubaidullin, G. Kolb, A. Theerthan

Division of Nuclear Power Safety
Royal Institute of Technology
100 44 Stockholm, Sweden

May 19, 2000

Contents

Sammanfattning	iii
Abstract	v
1 Introduction and background	1
1.1 Introduction	1
1.2 Background	1
1.2.1 Melt-water interactions	2
1.2.2 Corium spreading and coolability	3
1.2.3 Melt-vessel interactions during late phase of in-vessel core melt progression	5
1.3 Research objectives and approaches	7
1.3.1 Melt-water interactions	7
1.3.2 Corium spreading and coolability	7
1.3.3 Melt-vessel interactions during late phase of in-vessel core melt progression	8
2 Facility development	10
3 Research program description and results up to December 31, 1999	16

3.1	A selected list of papers published during 1999	16
4	Summary of the research results	18
4.1	Molten-fuel-coolant interaction (MFCI)	18
4.1.1	Test performance	19
4.1.2	Experimental results	19
4.2	Corium spreading and coolability (CSC)	22
4.2.1	Melt spreading	22
4.2.2	Re-spreading	26
4.2.3	Coolability of a particulate debris bed - POMECO program	27
4.2.4	Debris coolability by bottom injection	28
4.3	Melt-vessel interaction (MVI)	30
4.3.1	Natural convection in a stratified pool - SIMECO Program	30
4.3.2	FOREVER experimental program	34
5	Concluding remarks	37
	Bibliography	39

Sammanfattning

Detta är den årliga rapporten om det arbete som under 1999 utförts i forsknings-projektet MSWI (Melt Structure Water Interactions) som är en del av APRI-projektet och som finansieras av SKI, HSK, USNRC samt de svenska och finska kraftföretagen. Tyngdpunkten har legat på fenomen och egenskaper som styr fragmentering och sönderdelning av smältstrålar och smältdroppar, smältors utbredning och kylbarhet, samt termiska och mekaniska belastningar på ett tryckkärl p g a växelverkan mellan smälta och tryckkärl. Resultaten av många av de undersökningar som utförts i projektet har publicerats och presenterats i internationella tidskrifter och konferenser.

Vi anser att betydande tekniska framsteg har nåtts under dessa studier. Det har visat sig att:

- kylmedlets temperatur har en signifikant inverkan på karaktären hos fragmenten som bildas genom sönderdelningen av en oxidisk smältstråle. Vid låg underkylning är fragmenten relativt stora och oregelbundna jämfört med de mindre partiklarna som bildas vid hög underkylning.
- smältstrålens densitet har en avsevärd effekt på fragmentstorleken. Då smältans densitet ökar blir fragmentstorleken mindre. Medelmassan hos partiklarna i grusbädden ("debris") ändras proportionellt mot kvadratroten av kvoten mellan kylmedlet och smältans densitet.
- smältans överhettning har liten inverkan på fördelningen av storleken på de partiklar i grusbädden som bildas genom smältans fragmentering.
- smältstrålens anslagshastighet har en signifikant inverkan på fragmenteringsprocessen. Vid lägre hastighet, agglomereras (hopklumpas) smältans fragment och bildar en kaka av stora partiklar, s k "grusbädd". När hastigheten ökar, erhålls en mer fullständig fragmentering.
- skalningsmetodiken för smältans utbredning som utvecklades under 1998, har ytterligare validerats mot nästan alla tillgängliga experimentella data.
- experimentresultat för värmeflödet från homogen grusbädd vid torrkokning ("dry-out") med insprutning av vatten uppifrån överensstämmer väl med Lipinskikorrela-

tionen. För en skiktad grusbädd, dominerar det övre tunna skiktet med finare partiklar torrkokningsprocessen.

- resultat från experiment visar att fallspalten kan förhöja värmeflödet vid torrkokning med 50
- observationer från experiment visar att skiktning och blandning i smältpölen har stor effekt på fördelningen av värmeflödet i reaktortankbotten.
- FOREVER-testen i skala 1:10 ger nya och unika data för högtemperatur, multi-axiell krypdeformation av det prototypiska reaktortryckkärlet och för värmeöverföring genom egenkonvektion i en hemisfärisk smältpöl.

Acknowledgement: The appendix of this report consists of 9 technical papers published during 1999. These papers can be obtained from Nuclear Power Safety Division of Royal Institute of Technology by contacting:

Dr. Zhilin Yang
Nuclear Power Safety Division
Royal Institute of Technology
Drottning Kristinas Väg 33A
10044 Stockholm, Sweden
Teln. 46 8 790 9254, Fax. 46 8 7909197
E-mail: yang@ne.kth.se

Abstract

This is the annual report for the work performed in 1999 in the research project "Melt-Structure-Water Interactions During Severe Accidents in LWRs", under the auspices of the APRI Project, jointly funded by SKI, HSK, USNRC and the Swedish and Finnish power companies. The emphasis of the work is placed on phenomena and properties which govern the fragmentation and breakup of melt jets and droplets, melt spreading and coolability, and thermal and mechanical loadings of a pressure vessel during melt-vessel interaction. Many of the investigations performed during the course of this project have produced papers which have been published in the proceedings of technical meetings.

We believe that significant technical advances have been achieved during the course of these studies. It was found that:

- The coolant temperature has significant influence on the characteristics of debris fragments produced from the breakup of an oxidic melt jet. At low subcooling the fragments are relatively large and irregular compared to the smaller particles produced at high subcooling.
- The melt jet density has considerable effect on the fragment size produced. As the melt density increases the fragment size becomes smaller. The mass mean size of the debris changes proportionally to the square root of the coolant to melt density ratio.
- The melt superheat has little effect on the debris particle size distribution produced during the melt jet fragmentation.
- The impingement velocity of the jet has significant impact on the fragmentation process. At lower jet velocity the melt fragments agglomerate and form a cake of large size debris. When the jet velocity is increased more complete fragmentation is obtained.
- The scaling methodology for melt spreading, developed during 1998, has been further validated against almost all of the spreading experimental data available so far.
- Experimental results for the dryout heat flux of homogeneous particulate debris beds with top flooding compare well with the Lipinski correlation. For the stratified particle beds, the fine particle layer resting on the top of another particle layer dominates the dryout processes.

- Experimental results show that a downcomer may increase the dryout heat flux by 50% to 350%.
- The experimental observations show that stratification and mixing in the pool have profound effect on the heat flux distribution on the pressure vessel lower head.
- The FOREVER test provides at 1/10th scale new and unique data for high-temperature multi-axial creep deformation of the prototypical reactor pressure vessel, and for natural convection heat transfer in a hemispherical melt pool.

Chapter 1

Introduction and background

1.1 Introduction

This report describes the studies performed at the Division of Nuclear Power Safety of Royal Institute of Technology (RIT/NPS) during 1999 on melt-structure-water interactions that occur during the progression of a core melt-down accident. These studies, which began in 1994, are sponsored by a consortium consisting of Statens Kärnkraftinspektion (SKI), the Swedish and Finnish power companies (Vattenfall Ringhals, Forsmark Kraftgrupp AB, OKG AB, Barsebäck Kraft AB and TVO), the United States Nuclear Regulatory Commission (USNRC), the Nuclear Safety Commission of Switzerland (HSK), and the NKS project. Part of the work performed was reported, previously, and published as an NKS project report [1] and as SKI reports [2], [3], [4], [5], [6].

1.2 Background

The work performed at RIT/NPS during 1999 consists of three parts:

1. phenomena of melt-water interactions, with particular emphasis on fragmentation of a high temperature oxidic melt jet falling into water
2. corium spreading efficiency and coolability of ex-vessel debris beds
3. thermal and structural behavior of a pressure vessel during core melt-vessel interactions

1.2.1 Melt-water interactions

Fuel-coolant interactions (FCIs) may occur during the course of a severe accident in a light water reactor (see e.g. Theofanous, 1995 [7]). The nature of FCIs can range from benign film boiling to explosive interactions. Four distinct phases are thought to occur during an explosive FCI: pre-mixing, triggering, propagation (or fine fragmentation), and expansion phases (see a review by Corradini et al., 1988 [8]).

Several studies on jet fragmentation under MFCI conditions have been performed in the past using wide variety of simulant materials as well as prototypic corium as jet fluid as described in the studies by [9], [10] and [11]. Several analytical models and computer codes were developed based on linearised analysis of jet surface perturbations [9]. Both isothermal hydrodynamic jet fragmentation and boiling mode fragmentation of a melt jet in a volatile coolant were investigated. Although considerable progress has been achieved in explaining both the premixing and expansion phases of such interactions, there remain substantial uncertainties related to the initial MFCI process, which includes melt jet breakup, droplet formation, stripping and subsequent fragmentation, as well as thermal effects related to radiative heat transfer, film boiling and material solidification of mushy zone material. A recent review is provided by Turland [12]. This work is concerned with the high-temperature oxidic melt jet fragmentation and the resulting particle size distributions, which are important for debris formation and subsequent debris coolability.

The experimental program on melt jet fragmentation in a coolant is being performed at the Division of Nuclear Power Safety at the Royal Institute of Technology (RIT/NPS). The aim of the program is to develop an understanding of the effect of melt physical properties on the MFCI processes, based on simulant material experiments and to couple the results of these experiments with CFD modelling and analysis, see [13] and [16]. Dinh [14] and Haraldsson [15] reported results of previous low temperature experiments in which a variety of jet/coolant fluid pairs were employed to delineate the effect of melt physical properties on the fragmentation behaviour. These studies indicated that the size of the debris particles stripped from the jet body are highly dependent on the coolant temperature. Significant changes were also observed when the jet diameter was varied. Furthermore, insertion of an helical coil into the jet tube enhanced the jet turbulence level and showed a corresponding increase in the atomisation pattern.

Numerical simulations revealed that macroscopic momentum exchange between the jet and the coolant determines the jet fragmentation behaviour. Further refinement and validation of the models required an extended database which include the axial and lateral transport of melt and particle cloud as well as the characteristics of the particle bed formed.

1.2.2 Corium spreading and coolability

Corium spreading

For the next generation of nuclear power plants core melt scenarios have to be taken into account in the design. In the case of a reactor pressure vessel (RPV) melt through, measures have to be devised to stabilize the core melt, within the containment, in order to maintain its operability as the final barrier to fission product release. One promising solution is to provide a large spreading area for the melt ejected from the RPV to ensure that its thickness is thin enough to be coolable. This is the favored solution for the development of the French-German design of the European Pressurized water Reactor (EPR).

The Nuclear Power Safety division at KTH was a partner in a Joint Work Programme on "Corium Spreading and Coolability" (CSC) sponsored by European Commission during 1996-1999. The main objectives of this programme were to develop a sound scientific and technical basis to support the European nuclear industry, taking into account the results given by the CSC project and the design of reliable core-catchers. The project concentrated on: spreading of corium under both dry and wet conditions, and cooling of corium by direct water contact based on flooding from the top or from the bottom.

A number of experiments have been performed to study the phenomenology of core melt spreading on the containment floor (SPREAD, CORINE, BNL, VULCANO, KATS, COMAS, FARO, RIT/S3E). The main objective of these experiments was to provide data and observations for model development and validation. In particular, experimental programs conducted at JRC (FARO), Siempelkamp (COMAS), RIT (S3E), CEA (VULCANO) and FZK (KATS) are related to verification of the EPR melt retention scheme. Despite their non-prototypicalities (small scales, low temperatures, simulant materials, spreading channel geometry), the experiments provided invaluable insights into the physics of core melt spreading. In the KATS experiments, it was observed that even though the various (un-coated, coated, dry, wet) concrete spreading surfaces are somewhat different from that of ceramic, the spreadability i.e. spreading length is comparable. In addition, the presence of shallow water was found to have no detectable influence on spreading for high pour rate melt discharges. In the COMAS experiments, it was observed that the spreading distances were similar in channels with steel, ceramic and concrete substrate. The oxidic core melt was found to spread very well even when the melt superheat was small (up to 50K in FARO L-26) or even zero or negative (in COMAS 5a).

An initially spread-and-stopped, and crusted, mass (layer) of corium may re-spread earlier than it would get buried into the concrete substrate. There is the race: the internally-heated corium mass can break the crust and re-spread in the X-Y plane, or keep ablating the concrete and go downward (-Z) direction.

Much work has been performed on the concrete ablation of a crusted mass of melt (MACE tests at ANL, hot solid test at SANDIA etc.) The data from MACE provides the rate of downward ablation of corium into concrete at various temperatures of the crusted

melt pool. So far, however, no report has been found on the study of re-spreading phenomenon.

Ex-vessel corium coolability

Ex-vessel melt (debris) coolability is a critical safety issue for the current and the future light water reactor plants, with respect to management, and termination, of a postulated severe (core melt) accident. After vessel failure, the core melt pool attacks the concrete basemat, whose ablation can be terminated only by cooling the melt to below the concrete dissolution temperature.

The most convenient accident management measure to cool the melt is to establish a water layer on top of the melt pool. This coolability scheme has been investigated in the MACE experiments [17], where it was found that a tough crust is formed on the upper surface of the melt pool, which limits the access of the water overlayer to the melt. The conduction heat transfer through the thickening (with time) crust is insufficient to remove the decay heat generated in the melt. Another mechanism, i.e. melt eruption (like a volcano) into water, helps to remove some of heat; however achieving melt coolability below the concrete solidus temperature may take a considerable time, during which the melt keeps eroding the concrete basemat. Melt quenching was not achieved in any of the MACE experiments.

Achieving coolability by injecting coolant into the bottom surface of the core melt pool has been investigated in the COMET experiments at Karlsruhe [18]. In this scheme, water nozzles are embedded in the containment floor below its surface. Decay-heated core melt ablates through a sacrificial concrete layer before it reaches the water nozzles. The nozzles open as they contact the melt, thereby starting the water injection into the bottom of the melt pool. The COMET experiments using thermite melt and using prototypic core melt were performed at FZK and at ANL, respectively. In all cases, the melt was found to quench, in a relatively short time, to a porous, easily penetrable, debris with continued access of water to all regions of the previous melt pool. Engineered backfits or new designs based on the COMET scheme, however, appear complicated for implementation, and difficult to verify, in either existing or new plants.

Becker [19] performed experimental investigations on debris bed coolability by introducing vertical tubes, with slots at the bottom end, into the debris bed. These tubes acted as downcomers to channel water from an overlying water pool to the bottom region of the bed. In this approach the limitations associated with counter current flows of steam and water in a porous bed are avoided. Significant enhancement of dryout heat fluxes was found. In this scheme, even a stratified debris bed of small particles, resting on top of the bed of larger particles, was found coolable. The database, and related theoretical background developed, are, however, not sufficient to support a design modification incorporating downcomers in a containment to enhance debris coolability.

1.2.3 Melt-vessel interactions during late phase of in-vessel core melt progression

During the course of a hypothetical severe accident in a light water reactor (LWR), large amounts of molten core materials may be relocated to the reactor pressure vessel (RPV) lower plenum. Depending on accident scenarios, reactor design and accident management procedures, the in-vessel debris configuration may be different, fig.1.1. In general, the heat, transferred from the debris to the vessel, will cause the vessel heat-up and weaken the vessel. The lower head wall may be subjected to significant thermal and pressure loads, and is liable to failure due to melting or creep rupture (fig.1.1). For assessment of the consequence of severe core meltdown accident progression, the mode, timing and size of vessel failure is of paramount importance.

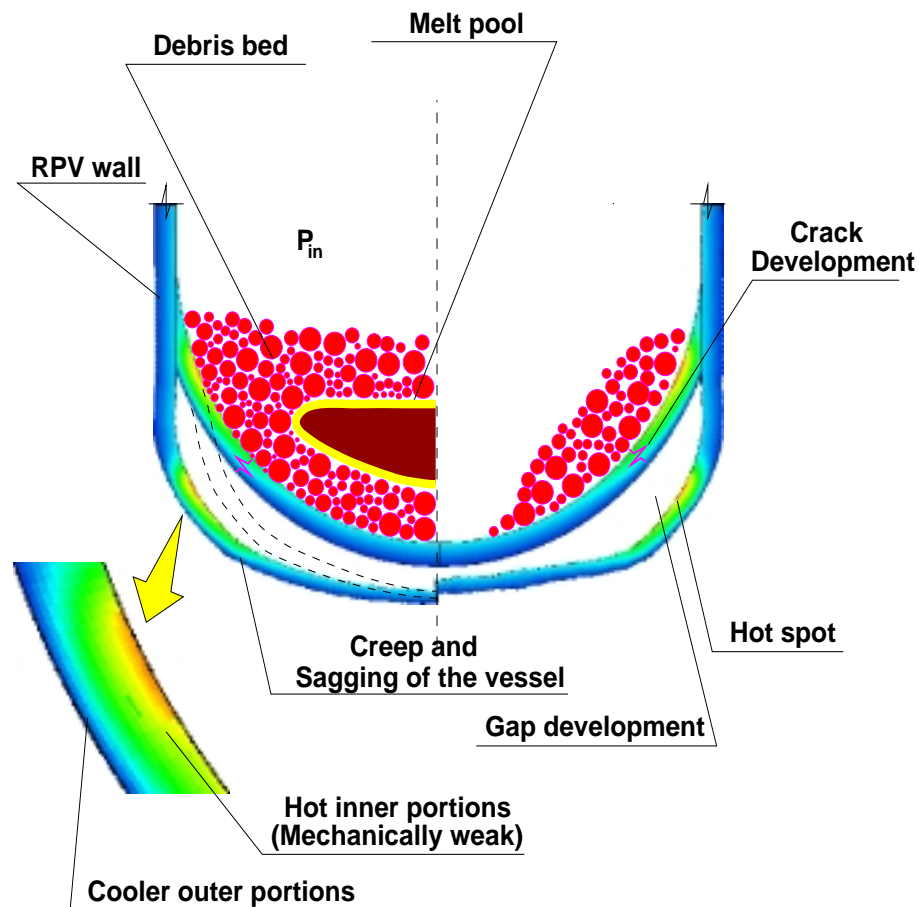


Fig. 1.1: Phenomenology of global and local creep rupture.

It was proposed recently, that the access of the water in the reactor lower plenum to the hot vessel wall prevented the TMI-2 vessel failure. The vessel gap cooling is proposed as an efficient mechanism of keeping the vessel wall cool and preventing vessel failure. The success of this mechanism largely depends on *a*) whether a gap is formed and maintained between the corium melt crust and the creeping vessel and *b*) whether water can penetrate into the gap to cool the vessel. Since the core melt relocation, debris bed formation, crust

formation and vessel creep are highly three-dimensional process, it is difficult to a priori predict the existence of the gap and of the pattern of water channeling in-between the vessel wall and the debris. Another important question is whether gap thermal hydraulics allows water ingress to sufficient depth to cool the lowermost regions of the vessel, and prevent its creep failure.

An overview of analytical and experimental investigations of creep rupture can be found in [22]. It is shown in [22] that the currently-existing numerical and analytical methods are prone to large number of uncertainties when assessing both the creep deformation and the time to rupture of the vessel for prototypical geometry and thermo-mechanical loadings. Only data from a limited number of experiments are currently available. Uniaxial tensile tests have been performed for different reactor vessel steels in the USA, Russia, Germany and France. So far, only a few multiaxial experiments investigating creep rupture of the reactor carbon steel at high-temperature conditions have been accomplished. In the RUPATHER experimental program, *e.g.*, a simple thin shell tube was subjected to internal pressure and axial-gradient thermal loading (temperature up to 1000°C). The data obtained in this experiment may be used for validation of different structural mechanics models. Recently, the LHF (Lower Head Failure) experiments have been performed at SNL, investigating creep failure of relatively large vessels (1/5th-scale), held at a pressure of about 100 bars, while the vessel bottom head is heated to temperatures of about 1000K [23]. The energy transfer to the reactor vessel from the core debris is simulated using a hemispherical resistance heater. Effects of peaking in the local distribution of heat transfer, and the impact of penetrations on the vessel failure time were the major focus of the LHF-1,2,3,4 experimental tests.

The current FOREVER program includes three major test series [24] [25] [26]. In the first series, we investigate the vessel deformation and creep behavior under thermal attack by naturally-convecting oxidic-melt pool (FOREVER/C series). The focus is placed on physical mechanisms which may govern the debris-vessel gap formation. In addition, data will be obtained on the creep rate at several locations on the lower head, which could be employed for validation of creep models and codes. In contrast to the SNL LHF experiments [23] (which simulate the TMI-2 scenario with 10 MPa pressure loading), the depressurized scenarios are the focus of the FOREVER tests. The second series FOREVER/G will be devoted to the gap cooling. Water will be supplied to the top of the melt pool after the vessel wall creep has occurred to a certain extent. Water ingress into the gap between the melt pool crust and the creeping vessel will be detected by thermocouples, mounted on the inner surface of the vessel wall. In the third series FOREVER/P, effects of penetrations on the vessel deformation and creep processes will be investigated.

The RASPLAV Program [27], employing prototypic ($\text{UO}_2\text{-ZrO}_2$) melt materials in a 200 kg slice facility, was performed to study the thermal loads imposed by the prototypic melt on a cooled vessel wall. The RASPLAV experiments, conducted at $Ra' \leq 10^{11} - 10^{12}$, have shown that the corium melt stably stratified in two layers with different composition and density. The lower layer was richer in UO_2 (heavier) whereas the upper was richer in ZrO_2 (lighter) which dramatically modified the heat flux distribution along the curved lower boundary.

There are very few studies reported in the literature on natural convection in two superposed fluids with internal heat generation. No computational or experimental studies of two stratified fluids with the upper one having a low, less than unity, Prandtl number, or of two superposed layers with different internal heat generation rates in both layers have been reported hitherto.

1.3 Research objectives and approaches

1.3.1 Melt-water interactions

The aim of research in this area is to investigate molten jet-coolant interactions, limited to the physical mechanisms which may govern instability and fragmentation of droplet and jet penetrating a coolant pool. Since the experimental database is rather meagre and uncertain, and the validity and applicability of different models is not so clear, a rational synthesis of the experimental information and calculation results aides in delineating various aspects of the underlying physics.

Differing from the work performed during the previous years, the major focus pursued in the work reported here is that of the melt physical properties on the fragmentation process of a melt jet. During 1999, a series of experiments of jet fragmentation with high temperature were performed, the objective of which was to observe and quantify the jet breakup characteristics, with emphasis on delineating the roles of melt physical properties and of coolant thermal-hydraulic conditions in the breakup process. In total, 22 experiments employing three high melting point binary oxides, $\text{CaO-B}_2\text{O}_3$, $\text{MnO}_2\text{-TiO}_2$ and $\text{WO}_3\text{-CaO}$ were performed. The melt jet was generated from a 25 mm nozzle and the velocity, which depends on the height of melt jet free fall, was varied up to 6 m/s. Melt mass of up to 35 kg ensured a long jet discharge time (up to 10s), thus, a quasi-steady jet breakup process.

1.3.2 Corium spreading and coolability

The objective of the Melt Spreading program at RIT is to develop the data base and modeling to predict the spreading efficiency of corium melt in the current LWR containments, in the melt spreading area of the EPR and in the new core catcher designs. Based on the experimental observations performed in RIT during 1997-1998, a scaling methodology for spreading efficiency was developed for both one-dimensional and two-dimensional open channels. The focus of our study on spreading during 1999 is placed on the validation, refinement and reactor applications of the scaling methodology developed in 1998.

The RIT method was first developed for spreading in one-dimensional channels [28], then was extended to cover spreading in two-dimensional channels and, more importantly,

for spreading into open area [29].

The experimental program of re-spreading was developed in 1999. The objective of this work is to develop a model which could describe the experiments well and then use it for prototypic accident situations. Experiments at intermediate temperatures have been performed to obtain data necessary for model development and validation.

The objectives of the research on corium coolability at RIT/NPS are

- to understand the physics which governs melt-coolant interaction and heat transfer in the bottom-injection coolability scheme;
- to investigate the potential of different cooling schemes for ex-vessel core debris.
- to assess the ability to cool deep debris beds of uniform and stratified configurations by a water overlayer.
- to assess if some back-fit devices, e.g. downcomers could be developed which would significantly enhance the coolability of deep uniform/stratified debris beds of relatively low porosity.

Two experimental programs have been developed, namely, DEbris COolability by Bottom Injection (DECOBI), and PORous MEDIA COolability (POMECA).

1.3.3 Melt-vessel interactions during late phase of in-vessel core melt progression

Two experimental programs, FOREVER and SIMECA, have been developed at RIT/NPS.

The objectives of the FOREVER tests are to obtain multiaxial creep deformation data for the prototypical vessel geometry (scaled 1:10), under prototypic thermal and pressure loading conditions. The distinguishable feature of the FOREVER tests, in comparison to the all previous LHF-1,...,8 (performed in Sandia NL) tests, is the high-temperature conditions of the vessel (950-1000°C vs. $\sim 700^\circ\text{C}$ in all LHF tests); and low-pressure-loadings (25 bars vs. 100 bars in the LHF experiments). In addition, the FOREVER test, is an integral experiment, which combines both melt pool natural convection and vessel creep deformation processes.

The SIMECA (Simulation of In-vessel MELt COolability) experimental facility was developed in order to investigate the effects of (i) boundary crust and mushy layer on natural convection heat transfer; (ii) melt stratification on natural circulation; (iii) turbulent flow on the possible amelioration of melt stratification; (iv) integral and multidimensional heat transfer between and in, the melt pool, the top metallic layer and the vessel. The work

performed during 1999 was focussed on the effect of, (i) the miscibility or immiscibility of the stratified layers, (ii) the density difference between the layers, (iii) the layer thickness and (iv) the heat generation in one or both layers. These investigations grew out of the findings in the RASPLAV Project that the melt pool could stratify into two layers. The change from homogeneous to stratified pool may significantly affect the thermal loading of the vessel wall.

Chapter 2

Facility development

During 1999, four new facilities were developed. They are DECOBI-HT (DEbris COolability by Bottom Injection - High Temperature), DECOBI-V (DEbris COolability by Bottom Injection - Visualization), POMECO (PORous MEDIA COolability) and SIMECO (Simulation of In-vessel MELt COolability) facilities.

Table 2.1 lists the main parameters for DECOBI-HT and DECOBI-V facilities.

Table 2.1: Test facility specifications

	DECOBI-HT	DECOBI-V
Dimension (cm)	I.D.= 20; H=50	B=60x30; H=100
Melt simulant	30%CaO + 70%B ₂ O ₃	water; paraffin oil
Melt temperature (°C)	1000-1200	25-250
Melt layer (cm)	8-20	10-40
Coolant	water	air; pentane
Number of nozzle	1-5	1-3
Diameter of nozzle (mm)	5	3-8
Measurement techniques	T;P;V	V

The schematic of the DECOBI-HT facility is shown in Figure 2.1. The DECOBI-HT facility consists of a cylindrical test section, a water supply system providing the water coolant to the test apparatus, an induction furnace producing the melt and a DAS (Data Acquisition System). With the exception of the DAS, the entire system was housed in a containment cell. All of the test apparatus is in modular form and the test section consists of 2 half cylindrical shells made of stainless steel sheet material (2.0 mm thick, 200.0 mm ID, 500.0 height). The nozzles for bottom coolant injection are connected to a lower plenum. These are made of steel material and copper pipes are used for their connection to the plenum. Thermocouples are inserted into the test section through the upper plate and

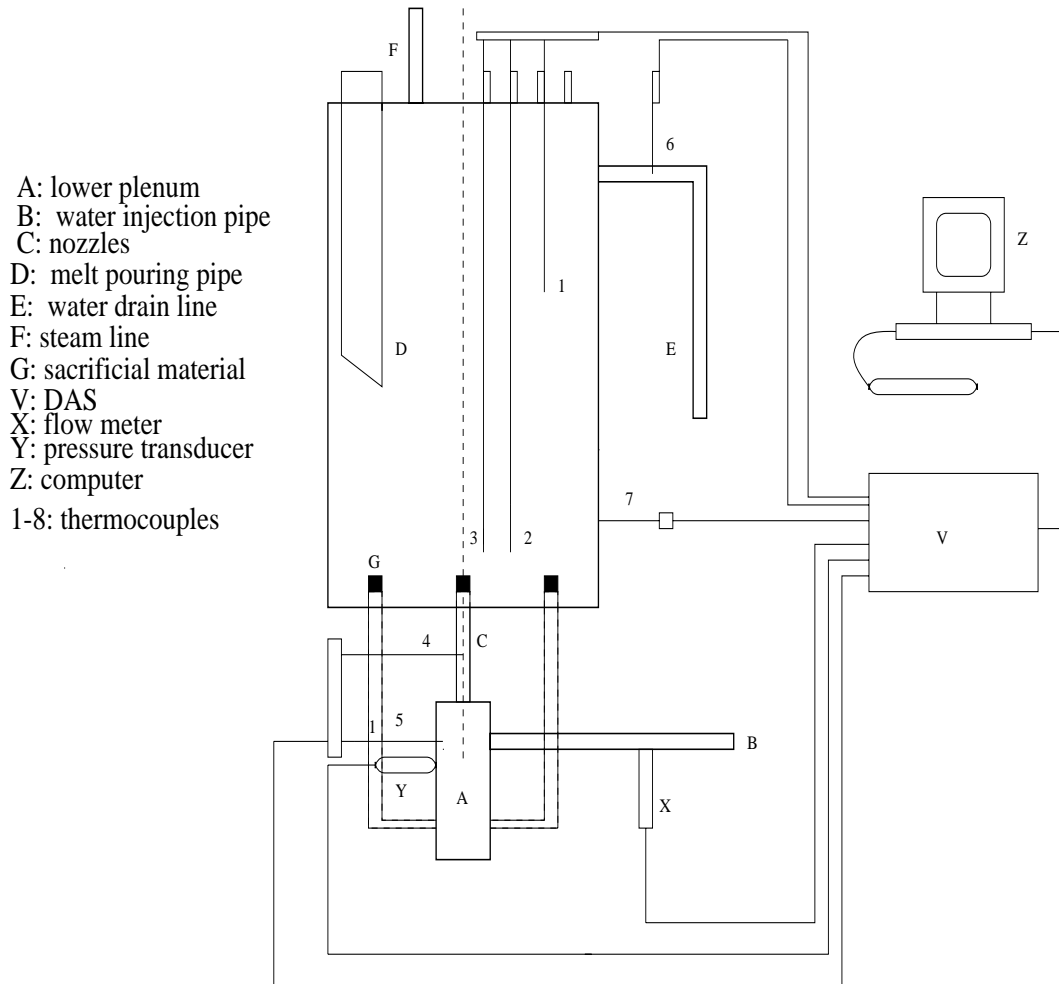


Fig. 2.1: DECOBI-HT Test Apparatus

are kept in place inside the test section with the help of guide lines in the upper plate (see Figure 2.1). Water is introduced into the test section through the lower plenum. The flow rate of water is recorded by a flowmeter.

The schematic of the DECOBI-V facility is shown in Figure 2.2. The test section is rectangular in cross section with dimensions: 30×60 cm, and with a height of 100 cm. Front and back sidewalls are made of glass, the lateral and bottom sidewalls are stainless steel. The nozzles, which are made of stainless steel, are connected through a lower plenum. The coolant is injected, for each test, at constant flow-rate. Different simulants for the coolant are employed in the experiments, which are supplied differently. The air is supplied to the test section by a compressor, through a pressure reducer and a flow meter. In the experiment performed using pentane, as coolant, a calibrated bottle is placed two meters higher than the nozzle level, so that a passive system is established. The average flow rate of pentane injected is calculated directly by measuring the liquid level variation in the bottle with time. The electric heater is installed in melt pool to obtain desired temperature. The whole process is visualized by a high speed digital video system comprising of a motion scope. The recording speed was kept at 250 frames/sec. The software OPTIMAS

was used to process the image pictures.

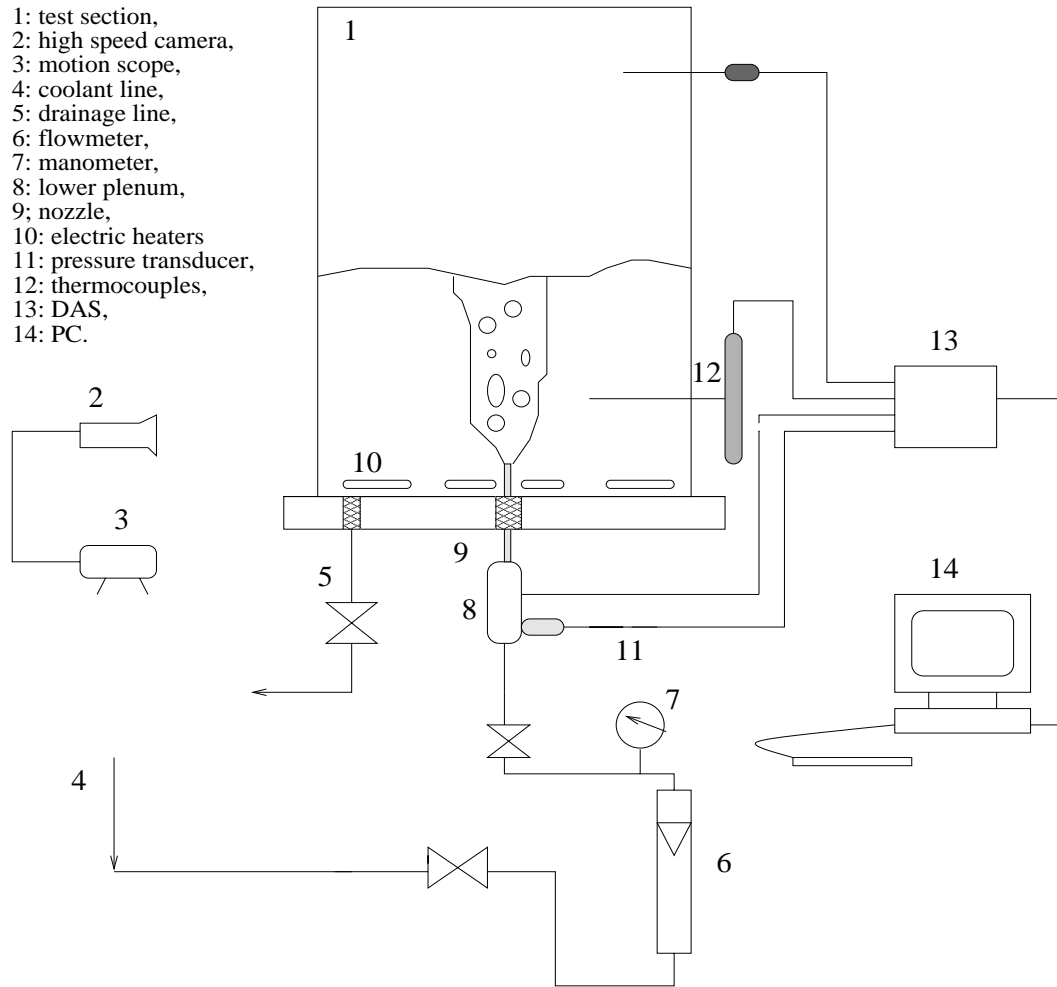


Fig. 2.2: DECOBI-V Test Apparatus

A schematic of POMECO facility, constructed in the laboratory of the Nuclear Power Safety Division (NPS) of Royal Institute of Technology (RIT), is shown in Figure 2.3. The POMECO facility consists of a water supply system, a test section, a heater system and a measurement and DAS systems.

The particle beds employed in the experiments are made of different sand samples, which have different mean particle size and porosity. Sand sample B is of 2-5 mm diameter with mean diameter of 4.01 mm and packing porosity of 0.405; Sample C is of 0.5-2 mm diameter with mean diameter of 0.92 mm and packing porosity of 0.375; and sample E is of 0-2 mm diameter with mean diameter of 0.198 mm and packing porosity of 0.38. We measured the porosities of different mixtures of these sand samples, and found that the mixture of sample B, C and E with mass ratio of 7:7:6 had the lowest porosity of 0.256. The top surface of the particle bed is covered by grids with small enough size to avoid channel formation in the particle bed and the flying-off of small size sand particles.

The test section is a stainless steel vessel of 350×350mm square cross-section and with

an upper and a lower part. The height of the lower part is 500 mm and the height of upper one 900 mm. The maximum height of 450 mm is available for the sand bed. A porous plate was placed 50 mm above the bottom of the test section to provide enough space for the distribution of water, coming from the downcomer, to the sand bed. The downcomer is a tube of stainless steel with 550mm height and 30 mm internal diameter, it is fixed on the porous plate. Before the sand bed is formed, a grid is placed on this porous plate in order to prevent fine sand particles from falling into the bottom space.

In the POMECO facility, the sand bed is heated internally by 22 resistance heaters with the maximum power delivery of up to 43KW.

The temperature of vapor generated in the test section is measured in the steam flow line, downstream the Vortex meter. The most important measurements in this experiment are the temperatures of the coolant and the sand bed. Thirty-three thermocouples are distributed in presentative positions of the particle bed. The outputs of these thermocouple are monitored carefully in order to determine the occurrence of the dryout.

The experiments are all performed at atmospheric condition. One pressure transducer ranging from 0 to 30 psi is installed downstream the vortex meter to measure the pressure of the steam to evaluate the mass flow rate of the steam generated in the particle bed.

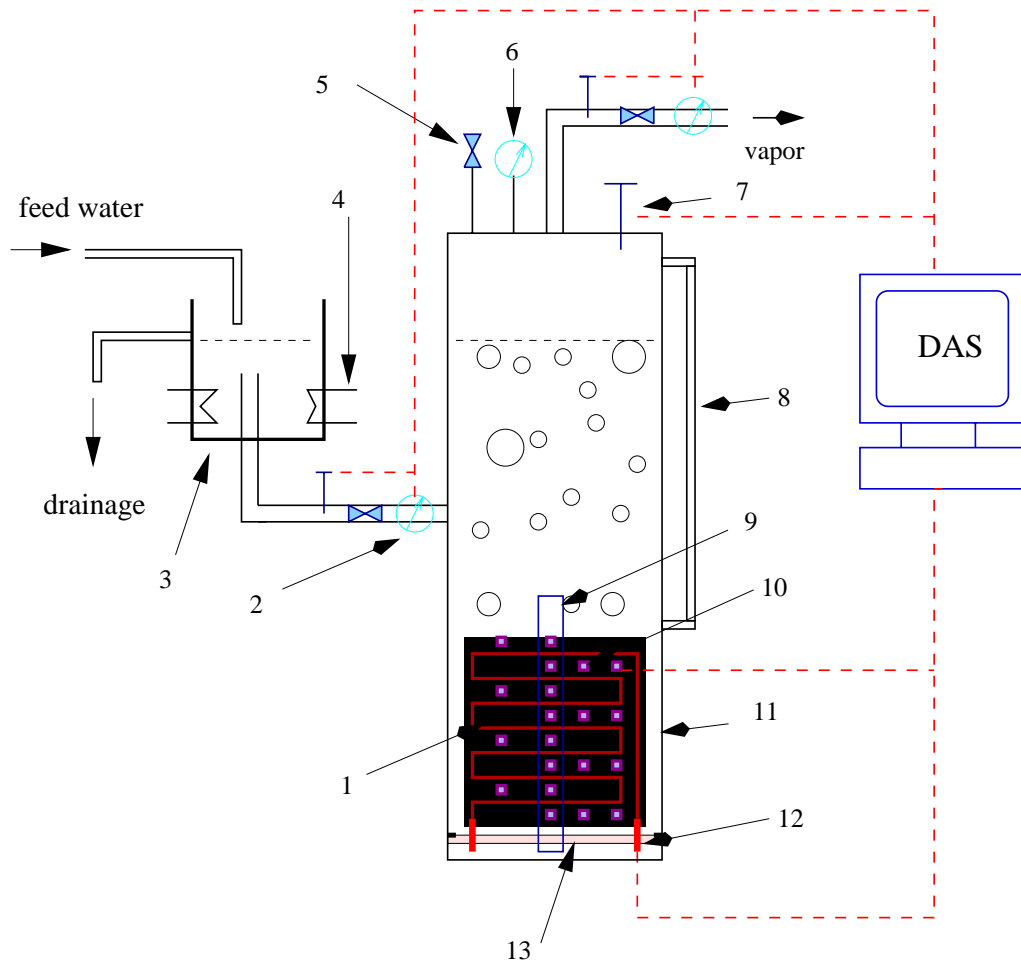
The steam flow rate is measured by a Vortex Flow Meter made by Omega Company, which is installed into the steam drain line (as shown in Figure 2.3). The range of this meter is up to 30 liter/sec. From the steam flow rate, we can evaluate the heat removal from the particle bed at the point of the dryout.

All the parameters mentioned above were sampled by using a HP data acquisition system. The sampling rate of 1 or 2 Hz is chosen.

The SIMECO facility consists of a slice-type geometry including a semi circular section and a vertical section. The diameter, height and width of the test section are 530x620x90mm (Figure 2.4). The slice walls are made of brass, except for the front wall which is made of a special glass allowing flow and crust visualisation. The vessel wall is cooled by controlled flow rate water loops (Figure 2.4). On the top of the pool a controlled flow rate water heat exchanger is used to provide the top boundary condition.

Internal heating in the pool is provided by thin cable-type heaters. Two heaters, 3-mm cable diameter and 4-m long are uniformly distributed in the semi-circular section. They can supply a maximum of 4 kW power to the pool.

Schematic of POMECO facility



- | | | |
|--------------|---------------------|-----------------|
| 1 Debris bed | 5 safety valve | 9 Downcomer |
| 2 flowmeter | 6 pressure gauge | 11 test vessel |
| 3 water tank | 7,10 TC | 12 heater |
| 4 heaters | 8 water level gauge | 13 porous plate |

Fig. 2.3: Schematic of the POMECO facility.

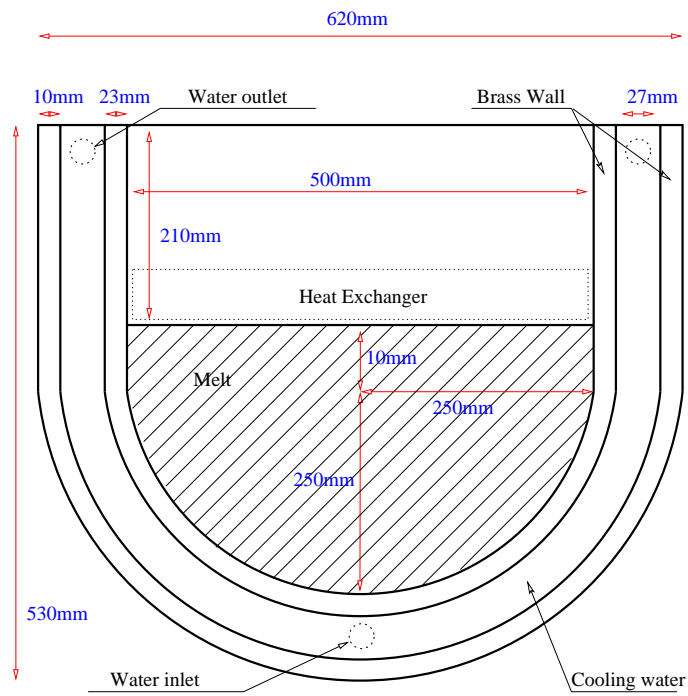


Fig. 2.4: SIMECO experimental facility - Main dimensions.

Chapter 3

Research program description and results up to December 31, 1999

The research program has resulted in many peer-reviewed publications. We are presenting here a selection which provides, (i) description of the experimental program and results on melt droplet-water interaction, melt jet fragmentation, corium spreading and coolability, vessel creep; and (ii) description of the analysis models and results dealing with the thermal hydraulic behavior occurring during the melt-water interaction, spreading, debris bed coolability, and melt-vessel interaction processes. Reprints or pre-prints of nine papers, whose particulars are listed below, are attached in this report.

3.1 A selected list of papers published during 1999

1. H.O. Haraldsson and B.R. Sehgal, Breakup of high temperature oxide jet in water, CD-ROM Proceedings of NURETH-9, San Francisco, California, Oct 3-8, 1999.
2. H.X. Li, V.A. Bui, T.N. Dinh and B.R. Sehgal, Numerical study of dynamics of melt drops in a liquid pool: focusing on the effect of gas-liquid interfaces, CD-ROM Proceedings of 33rd National Heat Transfer Conference, Albuquerque, New Mexico, Aug. 15-17, 1999.
3. M.J. Konovalikhin, T.N. Dinh and B.R. Sehgal, The scaling model of core melt spreading: validation, refinement and reactor application. OECD Workshop on Ex-vessel Debris Coolability, Karlsruhe, Germany, 16-18 Nov. 1999
4. G.J. Li, Z.L. Yang, H.X. Li and B.R. Sehgal, Analytical study of coolability of ex-vessel debris bed with downcomers, 4th International Symposium on Multiphase Flow and Heat Transfer, Xi'an China, August 22-24, 1999.
5. Z.L. Yang, M. Konovalikhin, G.J. Li, and B.R. Sehgal, Experimental investigation

on dryout heat flux of a particle debris bed with a downcomer, OECD Workshop on Ex-vessel Debris Coolability, Karlsruhe, Germany, 15-18 Nov. 1999

6. Z.L. Yang, R.R. Nourgaliev, T.N. Dinh and B.R. Sehgal, Investigation of two-phase flow characteristics in a debris particle bed by a Lattice-Boltzmann model, 2nd International Symposium on Two-phase Flow Modelling and Experimentation, Pisa, Italy, May 23-25, 1999.
7. D. Paladino, A.S. Theerthan, Z.L. Yang and B.R. Sehgal, Experimental investigations on melt-coolant interaction characteristics during debris cooling by bottom injection, OECD Workshop on Ex-vessel Debris Coolability, Karlsruhe, Germany, 15-18 Nov. 1999
8. B.R. Sehgal, R.R. Nourgaliev, T.N. Dinh, Characterization of heat transfer processes in a melt pool convection and vessel-creep experiment, CD-ROM Proceedings of NURETH-9, San Francisco, Oct. 3-8, 1999.
9. A.A. Gubaidullin, T.N. Dinh and B.R. Sehgal, Analysis of natural convection heat transfer and flows in internally heated stratified liquid pools, CD-ROM Proceedings of the 33rd National Heat Transfer Conference, Albuquerque, New Mexico, Aug. 15-17, 1999.

Chapter 4

Summary of the research results

The research work performed at RIT/NPS, within this project, can be divided into three parts, namely, 1) melt-fuel-coolant interaction, with particular emphasis on fragmentation of droplets and melt jets in water, 2) corium spreading and coolability, and 3) in-vessel thermal loading and vessel creep during core melt-vessel interaction.

In the first part, both experiments and analyses were performed. Innovative models of melt-water interactions were developed. A concept of melt jet fragmentation is proposed. Parametrics of melt physical properties were also investigated.

In the second part, experimental and analytical studies on melt spreading phenomena are presented. A scaling model is validated and refined against experimental data for different conditions. Experimental results on dryout heat flux of a particulate debris bed are presented. The experiments on melt coolability by bottom coolant injection under different conditions were performed.

In the third part, the first FOREVER experiment was performed and the results were analysed. The results on natural convection in the stratified internal-heated melt pool on SIMECO facility were analyzed.

4.1 Molten-fuel-coolant interaction (MFCI)

During 1999, a series of experiments of jet fragmentation with high temperature melt material were performed, the objective of which was to observe and quantify the jet breakup characteristics, with emphasis on delineating the roles of melt physical properties and of coolant thermal-hydraulic conditions in the breakup process. In total, 22 experiments employing three high melting point binary oxides, $\text{CaO-B}_2\text{O}_3$, $\text{MnO}_2\text{-TiO}_2$ and $\text{WO}_3\text{-CaO}$ were performed. The melt jet was generated from a 25 mm nozzle and the velocity, which

depends on the height of melt jet free fall, was varied up to 6 m/s. Melt mass of up to 35 kg ensured a long jet discharge time (up to 10s.), thus, quasi-steady jet breakup process. The detailed description of the experimental facility can be found in the attached paper No.1.

4.1.1 Test performance

At the beginning of each experiment the melt is prepared in the induction furnace. When the melt has reached the prescribed temperature the coolant tank is filled with water at a chosen temperature. The furnace is then tilted and the liquid melt is delivered to the funnel. The jet is instantly formed and discharges from the nozzle into the coolant pool. At the same time the data acquisition system (DAS) samples data from all the instruments. The procedure is repeated for other experiments at different temperatures of melt and coolant.

Three binary oxide mixtures CaO-B₂O₃, MnO₂-TiO₂ and WO₃-CaO served as the melt jet fluid: The compositions are 30% CaO-70% B₂O₃, 82% MnO₂- 18% TiO₂, 92.5% WO₃- 7.5% CaO weight percent, respectively.

In the twenty two experiments performed so far, sixteen experiments were performed with CaO-B₂O₃ melt, two experiments were conducted with MnO₂-TiO₂ melt and four experiments with WO₃-CaO melt. The first ten experiments were of scoping nature with limited instrumentation, the others are fullscope experiments performed with larger melt mass and complete instrumentation.

Note that some of the tests were repeated under identical conditions in order to ensure reproduction of the observation and data. The first two experiments were performed with 0.4m falling height whereas the rest of the experiments were performed with a falling height of 1.4m.

4.1.2 Experimental results

Jet dynamics

Figure 4.1 shows the transient behavior of the jet as it penetrates into the coolant pool. It was observed that soon after entry into water the jet undergoes significant fragmentation due to atomization. The Weber number, $\frac{\rho_c |U_j - U_c|^2 D_j}{\sigma}$, based on relative velocity between jet and coolant, is high during this period and may reach values of 5×10^3 . The temperature of the coolant pool significantly affects the initial jet dynamics and its breakup behaviour. It is observed that coolant boiling is quite violent for subcooled conditions. This has significant influence on the initial jet dynamics.

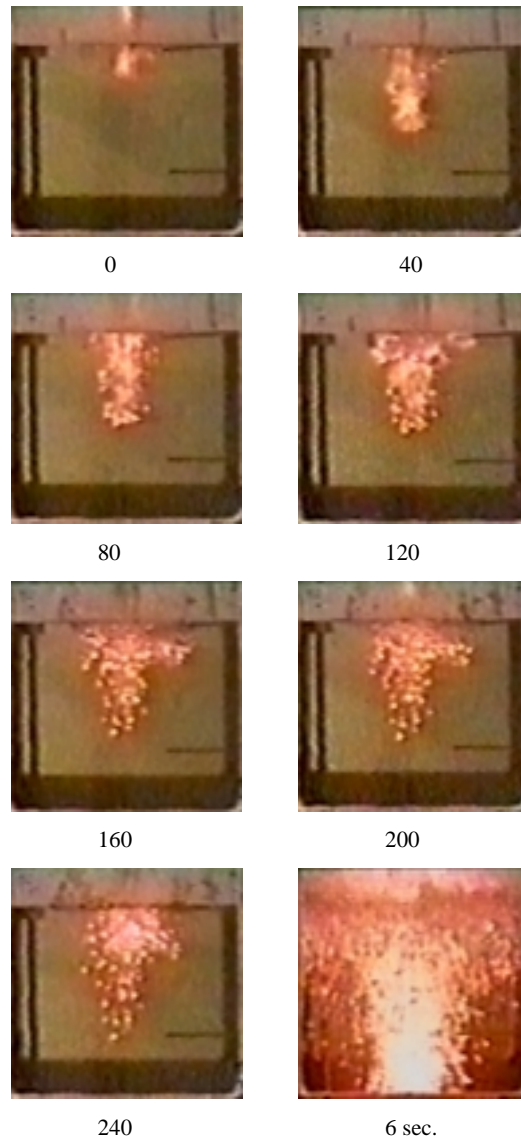


Fig. 4.1: Jet fragmentation dynamics. Jet diameter 25 mm, jet velocity $U_j^0=6$ m/s. Time between frames 40 ms, except last frame is 6 sec. into the process.

Effect of coolant temperature

The foremost results obtained from these experiments is that the melt jet fragmentation can be classified into two regimes of either *fragmentation-controlled* or *solidification-controlled*. The delineation between these two regimes can be realised from the size characterisation and morphology of the solidified debris which is formed. It was found that primary determinant of which regime the jet fragmentation would fall under was temperature of the coolant.

Figure 4.2 shows the typical morphology of fragments produced in the fragmentation-controlled regime. In this regime the jet breaks into a large number of irregular particles, coupled with very fine spherical particles. Conversely in the solidification-controlled regime, the melt jet breaks into large particles. The particles are smooth and often with

hollow cavity and very brittle. Figure 4.3 shows a typical morphology of particles in the solidification controlled regime.

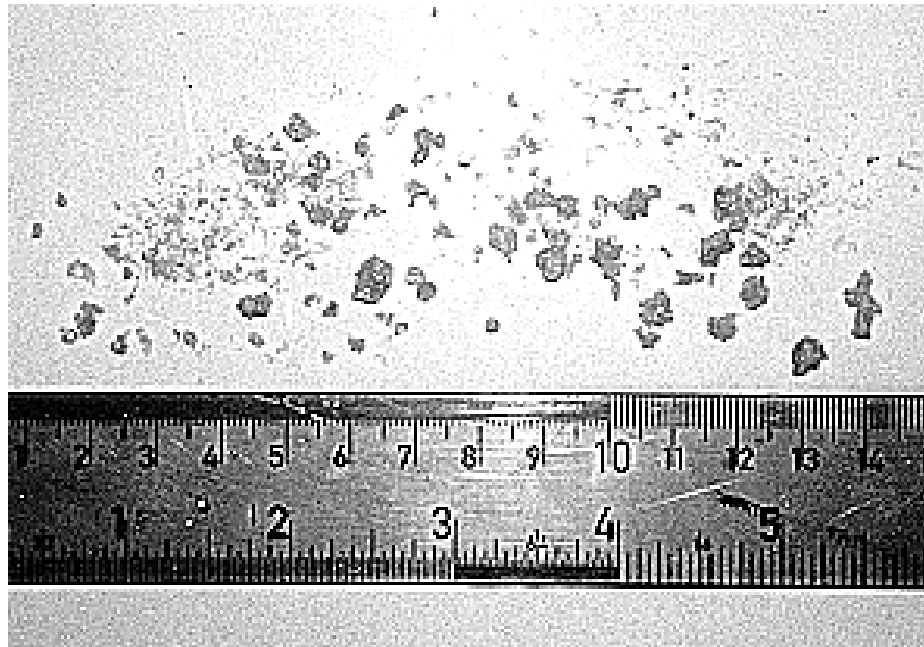


Fig. 4.2: *Typical morphology of the fragmentation debris in the fragmentation-controlled regime*

Another distinct difference between those two regimes is related to the particle size distribution of the debris produced. In the fragmentation controlled regime, particles of different size from 0.1 mm up to the maximum size are found in the debris. However, in the solidification-controlled regime, there are mostly large particles and only few small particles. This difference can clearly be seen in Figure 4.4, which depicts the cumulative mass-size distributions of the debris produced when $\text{WO}_3\text{-CaO}$ oxide jet interacts with coolant of different temperatures. In this figure, the curve with $T_w=25^\circ\text{C}$ corresponds to the fragmentation-controlled regime, while the curve with $T_w=95^\circ\text{C}$ corresponds to the solidification-controlled regime. At different coolant temperatures, the cumulative mass distributions are remarkably different.

Figure 4.5 shows the variation of the debris mass mean sizes with coolant temperature. A strong dependence of the mass mean particle size on the coolant temperature is observed for the $\text{WO}_3\text{-CaO}$ oxide. The lower the coolant temperature, the smaller the debris mass mean size. Obviously, Figure 4.4 and Figure 4.5 together show the strong effect of the coolant temperature on the droplet fragmentation process.

Effect of melt density

Cumulative mass distributions of the fragmented particles produced in the tests are compared in Figure 4.6. In this figure tests performed with three different material densities are included with the corresponding densities of 2500 kg/m^3 , 4300 kg/m^3 and 6500 kg/m^3 ,

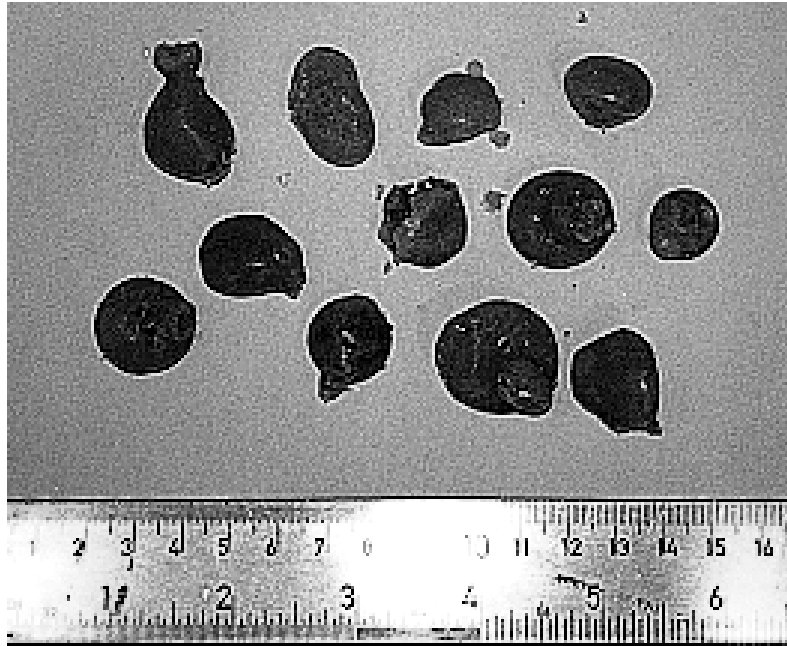


Fig. 4.3: *Typical morphology of the fragmentation debris in the solidification-controlled regime*

respectively. From Figure 4.6 it can be seen that for all three materials, the cumulative mass distributions are sensitive to the coolant temperature. It appears that as the melt density increases the smaller particles are produced during the jet breakup.

4.2 Corium spreading and coolability (CSC)

4.2.1 Melt spreading

Based on the experimental observations performed in RIT during 1997-1998, a scaling methodology for spreading efficiency was developed for both one-dimensional and two-dimensional open channels. The focus of our study on spreading during 1999 is placed on the validation, refinement and reactor applications of the scaling methodology developed in 1998.

The RIT method was first developed for spreading in one-dimensional channels [28], then was extended to cover spreading in two-dimensional channels and, more importantly, for spreading into open area [29].

In the RIT method, the terminal spread melt thickness is shown to be a function of the time scales of two competing processes: hydrodynamic (convective) spreading time scale and solidification time scale. In the gravity-inertia regime, the hydrodynamic spreading

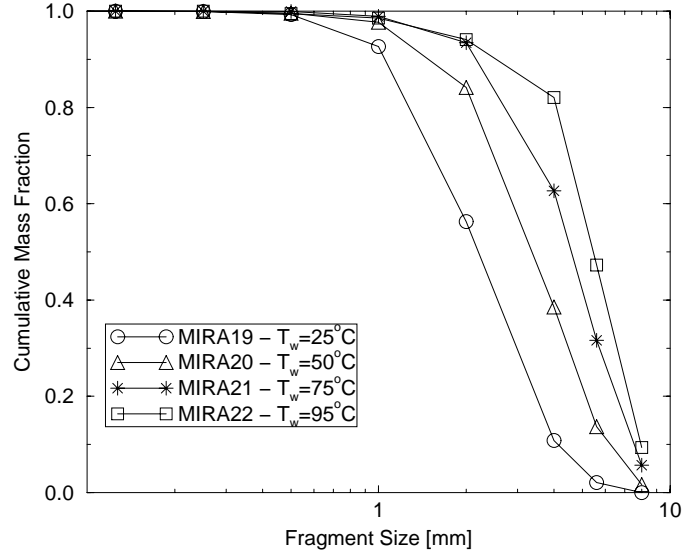


Fig. 4.4: *Dependence of the debris size distributions on the coolant temperature*

time scale is determined as the time period required for liquid (melt) to spread to reach its capillary thickness. The characteristic solidification time scale is defined as the time period needed to cool the melt to an immovable state. For this, not only the superheat, but also a fraction of the latent heat of fusion, has to be removed from the bulk melt.

Based on the mass and momentum conservation equations, a square-root relation was established between the dimensionless length scale (representing ratio of final spreading thickness to capillary thickness) and the dimensionless time scale (representing ratio of hydrodynamic spreading time to solidification time). The square-root law was shown to be valid in both gravity-inertia and gravity-viscous regimes, employing a dimensionless viscosity number, which was analytically derived.

One-dimensional model

The dimensionless time scale combines parameters of the process (V_{tot} , G , ΔT_{sup}), geometry (D), boundary conditions (h_{conv} , T_{env}) and melt physical properties (H_{fusion} , Cp_m , ρ_m , μ_m).

The dimensionless length scale \mathcal{L} represents a measurable (and highly reproducible) result of the spreading process (terminal spreading melt thickness, (δ_σ)).

In order to obtain one-dimensional scaling laws the dimensionless length scale \mathcal{L} was related to the dimensionless time scale \mathcal{T} .

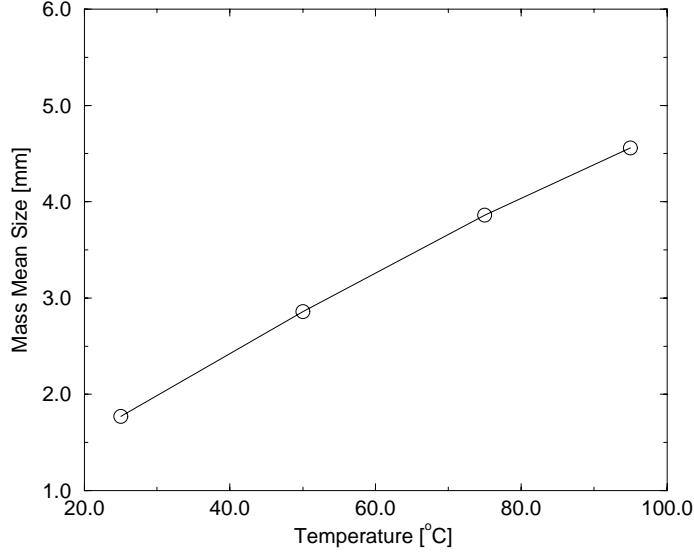


Fig. 4.5: Mass mean size of the debris from droplet fragmentation tests

Gravity-inertia regime:

$$\mathcal{L} = C \cdot \mathcal{T}^{1/2} \quad (4.1)$$

Gravity-viscous regime:

$$\mathcal{L} = C_v \cdot \mathcal{T}^{1/2} \cdot \mathcal{N}^{1/2} \quad (4.2)$$

where the viscosity number \mathcal{N} is defined as follows:

$$\mathcal{N} = \frac{\nu^{1/8} \cdot V_{tot}^{1/2} \cdot g^{5/24}}{D^{1/3} \cdot G^{13/24}} \quad (4.3)$$

Two-dimensional model

Based on observations from 2D melt spreading experiments the 2D scaling model was developed at RIT/NPS [34]. Several regimes of melt spreading into an open area were considered: hydrodynamics, open channel flow (OCF), thermo-controlled. It was found that a scaling rationale based on the open channel flow theory compares best to the measurements in the tests conducted at RIT.

Essentially, the scaling law for spreading into 2D area is based on the concept of melt spreading in 1D channel, with accounting for the reduced hydrodynamic time scale of the unbounded liquid on horizontal surface. Exactly similar procedure as for 1D spreading was applied for deriving the relation between the time and length scales. As a result, the general viscid form can be written as follows.

$$\mathcal{L} = C_\alpha \mathcal{T}^{1/2} \mathcal{B}^{1/2} \mathcal{N}^{1/2} \quad (4.4)$$

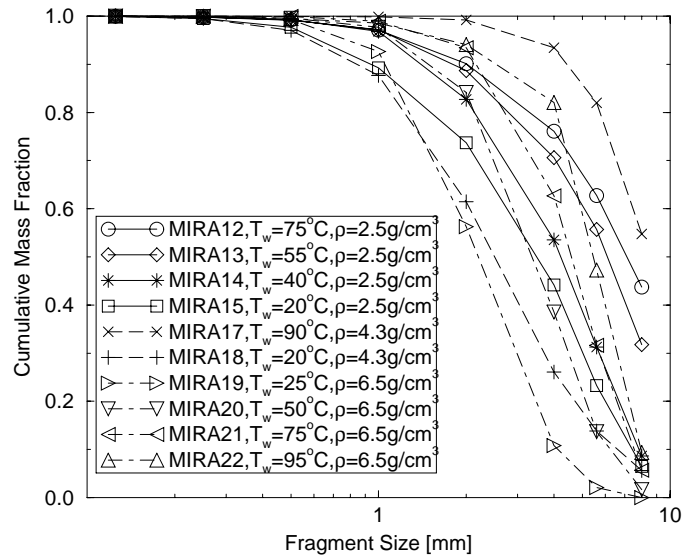


Fig. 4.6: *Effect of melt density on the debris size distribution*

Table 4.1: Parameter \mathcal{B} in 2D spreading model

	\mathcal{B}
hydrodynamic regime	$\frac{1}{1 + \frac{2R}{D_o}}$
open channel flow theory	$D_o \left(\frac{360\delta_{cap}}{\alpha_{ocf}\pi V_{tot}} \right)^{1/2}$
thermal-control regime	$\frac{1}{1 + \frac{2\tau_{solid}U_o}{D_o}}$

with parameter \mathcal{B} defined in Table 4.1.

The scaling relations were then shown to be capable of analyzing and even predicting results of melt spreading experiments, including those at relatively large scales and using prototypic core melts. A number of mechanistic equations and generic correlations were employed to enable closed form scaling equations for different regimes and geometries. As such the scaling equations serve as an integral model for assessing and predicting the terminal characteristics of melt spreading.

Validation against experimental data

The strategy adopted for validation of the melt spreading model includes:

- verification of component models and correlations which were employed as basis to develop the scaling methodology;
- validation of the integral model against data and observations in one-dimensional simulant-material melt spreading experiment;
- validation of the model against data obtained from two-dimensional simulant-material melt spreading experiments; and
- validation of the model against data obtained from high-temperature melt spreading experiments employing prototypic core melts.

Figure 4.7, 4.8 and 4.9, respectively, show the comparison of the prediction made with the scaling law developed above against the data obtained from almost all of the spreading experiments performed so far.

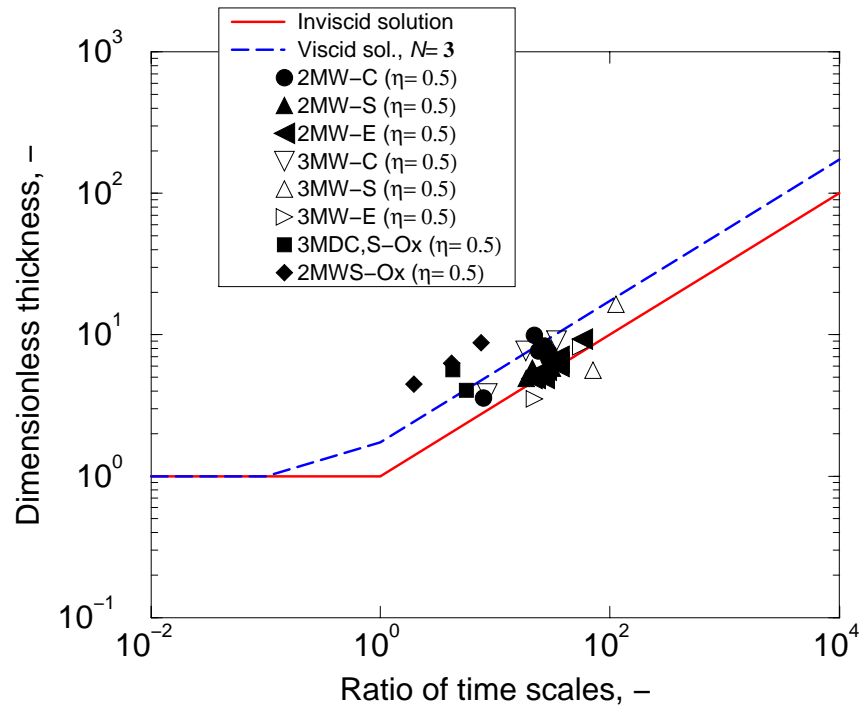


Fig. 4.7: One-dimensional spreading analysis with data obtained in RIT.

4.2.2 Re-spreading

The experimental program of melt re-spreading has been developed. As melt simulant a binary non-eutectic salt mixture: 20-80% NaNO_3 - KNO_3 was employed. The test facility was constructed, which consists of a rectangular cavity 299x200x100 mm occupied by a molten salt mixture with a vertical crust boundary. The resistance heater was used to

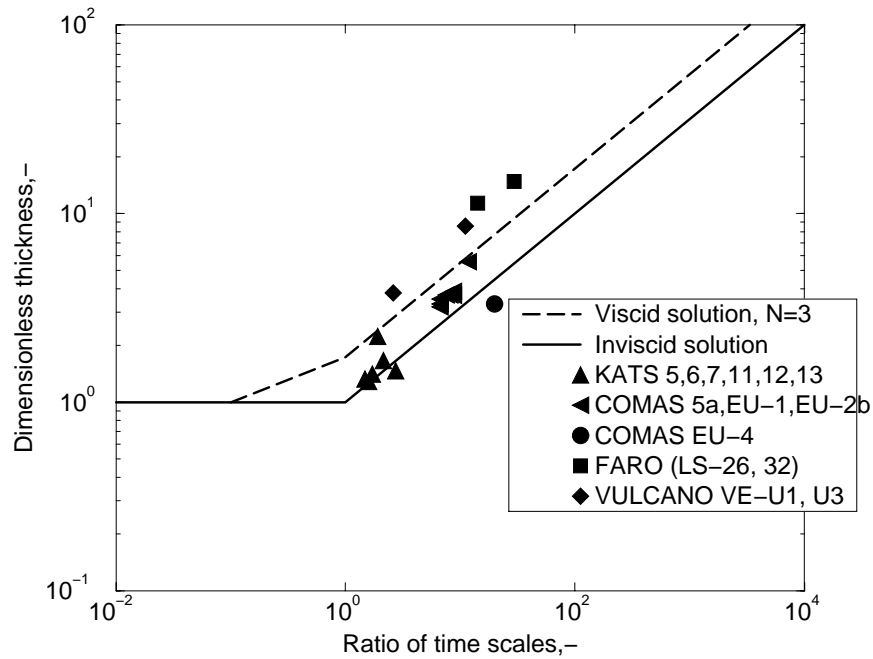


Fig. 4.8: One-dimensional spreading analysis with data obtained by other organizations.

maintain the internal-heating and to re-melt the simulant. Data was obtained on crust re-melting (break-up), its location and subsequent re-spreading of the melt.

A series of experiments were performed considering:

- different initial cooling times (different initial crust thicknesses)
- different power supply (different internal heat generation)
- different top boundary conditions (radiation or no radiation from the top)

Experimental observations show that in all tests the crust break location was at the upper part of the vertical crust layer and the governing mechanism of this phenomena is the melting of the crust driven by natural convection in the melt contained inside, as also observed in the TMI-2 accident. Analyses of experiments were performed with the MVITA code [30]. Experimental and calculated results are in reasonable agreement.

4.2.3 Coolability of a particulate debris bed - POMEKO program

Two series of experiments performed on the dryout heat flux with different configuration of the porous particulate bed have been described. One is with homogeneous beds, another

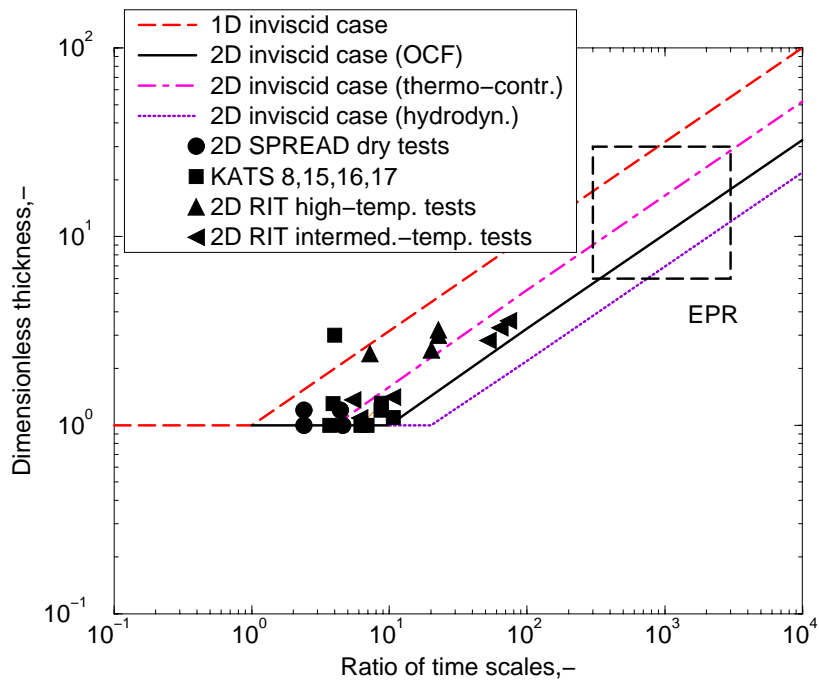


Fig. 4.9: Two-dimensional spreading analysis.

one is with stratified beds. The porosity of particle bed was varied from 25 to 40%, and the average particle size from 0.2 to 1 mm.

Tables 4.2 to 4.5 give the conditions and the results of the experiments for homogeneous and stratified particle beds, respectively.

Experimental results for the dryout heat flux of homogeneous beds with top flooding compare well with the Lipinski correlation. For the stratified particle beds, the fine particle layer resting on the top of another particle layer is found to dominate the dryout processes. The effect of a downcomer on the dryout heat flux was investigated for both homogeneous and stratified particle beds. The experimental observations show that the positions where dryout occurs for the bed with downcomer are always higher than those for the bed without downcomer. It was found that a downcomer may enhance the dryout heat flux from 50% to 350%.

4.2.4 Debris coolability by bottom injection

A series of experiments was performed using the non-eutectic oxide mixture $30\%CaO + 70\%B_2O_3$ ($T_{liq} = 1027\text{ }^\circ\text{C}$, $T_{sol} = 977\text{ }^\circ\text{C}$) as melt, and water as coolant on DECOBI-HT facility. The main experimental conditions and results are listed in Table 4.6.

Table 4.2: Experimental matrix for homogeneous particle beds.

Test Number	Sand Bed Type	Downcomer
Homo-1.1	Sand sample: 0-2mm diameter, Porosity = 0.397 $D_{mean} = 0.198\text{mm}$	No
Homo-1.2	same as Homo-1.1	Yes
Homo-2.1	Sand sample: 0.5-2mm diameter, Porosity = 0.365 $D_{mean} = 0.92\text{mm}$	No
Homo-2.2	same as Homo-2.1	Yes
Homo-3.1	Sand sample: sand mixture- $M_B:M_C:M_E=7:7:6$ Porosity = 0.258, $D_{mean} = 0.8\text{mm}$	No
Homo-3.2	same as Homo-3.1	Yes

M - mass fraction; Types of sand B: 2-5 mm; C: 0.5-2 mm; E: 0-2 mm

Table 4.3: Experimental results on dryout heat flux for homogeneous particle beds.

Test Number	Experiment KW/m ²	Lipinski model KW/m ²	Enhancement by downcomer
Homo-1.1	89.8	23.2	
Homo-1.2	183.0		103.8%
Homo-2.1	222.04	215.1	
Homo-2.2	331.42		49.26%
Homo-3.1	44.9	51.4	
Homo-3.2	202.04		348%

The experimental observations show that the structure and extension of the porosity region is strongly related to the initial melt conditions and the coolant conditions. The superheat of the melt is found to be one of the key parameters governing the porosity formation behavior. The case with low flow rate of the coolant and low superheat of the melt is shown in Figure 4.10a and it is seen that the overall porosity formed is very low, with two clear non-porous regions. For the case with higher coolant flow rate and higher melt superheat, the porosity structure is found to be branched-channel-like inside the debris (Figure 4.10b). The melt that interacts directly with the coolant is solidified very quickly, and the rigid structure formed prevents the remaining melt from contact with coolant. Those unquenched regions of the melt are cooled slowly by conduction. For the cases with five nozzles, with greater depth of melt (~ 20 cm) and high flow rate of coolant, the porosity structure was quite uniform (Figure 4.11) and branched-channels were observed. Two of the five nozzle cases did not produce much porosity. For these cases water at 90°C was injected in the melt pool.

On the DECOBI-V facility, single-phase and two-phase coolant jet behaviour for a wide range of experimental conditions in low and high viscosity pools have been studied. These

Table 4.4: Experimental matrix for stratified particle beds.

Test Number	Sand Bed Type	Downcomer
Strat-1.1	Upper layer: 0-2 mm, H = 130 mm Lower layer: 0.5-2 mm, H = 240 mm	No
Strat-1.2	same as Strat-1.1	Yes
Strat-2.1	Upper layer: sand mixture - $M_B:M_C:M_E=7:7:6$, H = 130 mm Lower layer: 0.5-2 mm, H = 240 mm	No
Strat-2.2	same as Strat-2.1	Yes
Strat-3.1	Upper layer: 0-2 mm, H = 240 mm Lower layer: 0.5-2 mm, H = 130 mm	No
Strat-3.2	same as Strat-3.1	Yes
Strat-4.1	Upper layer: sand mixture $M_B:M_C:M_E=7:7:6$, H = 240 mm Lower layer: 0.5-2 mm, H = 130 mm	No
Strat-4.2	same as Strat-4.1	Yes

experiments show that the expansion, fragmentation, and phase change of the coolant are strongly dependent on the viscosity of the melt pool. In the two-phase coolant experiments, it is seen that for low flow rate the coolant is fragmented into small bubbles readily which allows an increase in the vaporization rate. More experiments are undergoing, we believe that the data obtained would help to develop a parametric model describing the porosity formation process. Another series of experiments in a medium size test facility is also planned using different binary oxide melt simulant so that the effect of the melt properties on the processes of porosity formations and heat transfer can be understood.

4.3 Melt-vessel interaction (MVI)

4.3.1 Natural convection in a stratified pool - SIMECO Program

For uniform pool, water and binary salt mixtures are employed as melt simulants. Both eutectic mixture (50%-50%) and non-eutectic mixture (20%-80%) of $\text{NaNO}_3\text{-KNO}_3$ are used in the SIMECO experiments. The binary-mixture phase diagram is quite similar to that of the binary-oxide core melt $\text{UO}_2\text{-ZrO}_2$. For the 20%-80% mixture the temperature difference between the liquidus and solidus is about 60K. The liquidus temperature of the binary mixtures are 220°C and 280°C, respectively, for the 50%-50% and 20%-80% compositions. Previously, these salt mixtures were extensively, and successfully, employed as core melt simulants in melt-vessel interaction experiments performed at RIT/NPS [38]. The heat of fusion, heat capacity, density, viscosity, heat conductivity of these mixtures were measured

Table 4.5: Experimental results on dryout heat flux for stratified particle beds.

Test Number	Experiment, KW/m ²	Enhancement by downcomer
Strat-1.1	87.64	
Strat-1.2	186.77	113%
Strat-2.1	53.87	
Strat-2.2	138.28	157%
Strat-3.1	55.67	
Strat-3.2	190.36	242%
Strat-4.1	122.1	
Strat-4.2	235.26	92.6%

Table 4.6: Experimental Conditions and Results

TEST	Melt volume (liters)	Melt temp. (°C)	Coolant temp. (°C)	Coolant over press. (bar)	Coolant flow rate (liter/min)	Solidif. time (sec)	Porosity %
1N-I	3.6	1197	27	0.12	0.15	100	-
1N-II	2.5	1147	27	0.12	0.64	60	20
5N-III	2.5	1147	27	0.12	0.67	50	60
5N-IV	4.0	1157	27	0.13	1.50	30	41
5N-V	4.0	1157	90	0.20	1.20	90	16
5N-VI	4.0	1070	90	0.20	0.80	10	-
5N-VII	6.0	1157	27	0.80	1.50	30	38
5N-VIII	6.0	1157	27	0.20	2.30	20	44

to enable pre-test and post-test analyses of the experiments. For stratified pool, water and salt water (with different salt concentrations), as well as, parafin oil and water are pairs employed respectively, as simulant for stratification of miscible and immiscible fluids.

The water loop temperatures are used to obtain the average heat flux on the side wall and on the top of the pool. A total of 36 K-type thermocouples are kept inside the brass vessel wall at different angular locations in order to derive local heat fluxes. Inside the pool, 34 K-type thermocouples are installed to measure the local temperature variation, with emphasis on the near wall region and the interface between the two stratified layers. Video recording of the test section is used to track, for the uniform salt pool, the crust behavior, and for the stratified pool, the interface behavior and mixing process.

For the uniform pool, the SIMECO test matrix is designed to cover:

- different pool compositions;

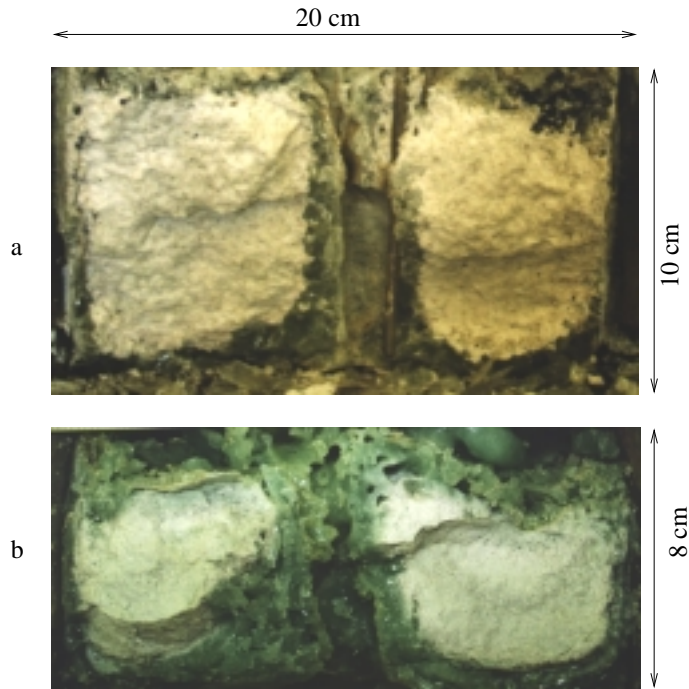


Fig. 4.10: DECObI-1N-I and II. Post Test Section

- different top and sidewall cooling conditions;
- different heat generation rates.

In a scoping test series, water was employed as melt simulant, while in the main test series, binary salt mixtures are employed. The SIMECO facility enables experiments with Rayleigh numbers up to $1.9 \cdot 10^{13}$ (with salt) or $5.5 \cdot 10^{13}$ (with water) for the pool natural convection. The flow fields are expected to be turbulent for these values of the Ra' .

For the stratified pool, the SIMECO test matrix is designed to cover:

- immiscible and miscible fluids;
- different upper layer thicknesses;
- different heat generation rates;
- one or both layers heated;
- different density difference.

During these experiments the Rayleigh number (Ra'), based on the lower pool, vary from $3.8 \cdot 10^{11}$ to $5.5 \cdot 10^{13}$.

Uniform pool test series

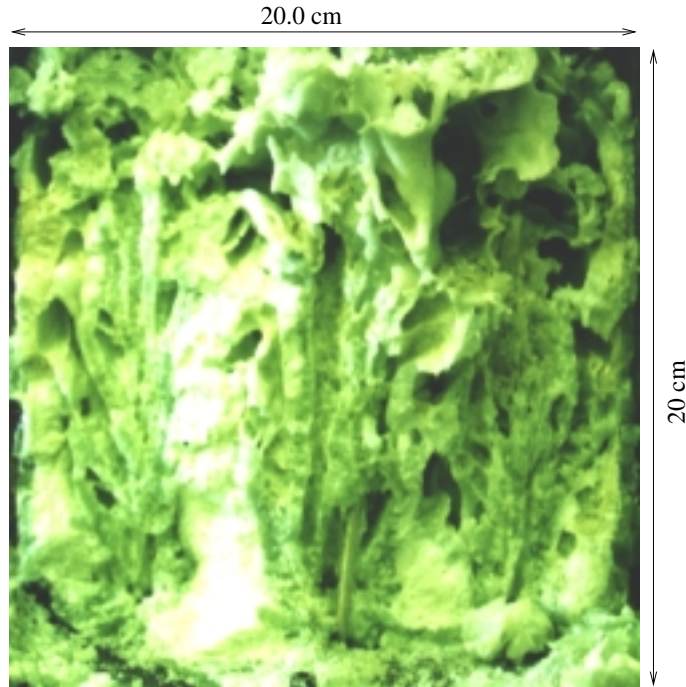


Fig. 4.11: DECOBI-5N-VII. Post Test Section

The steady state regime is characterized by two distinct zone in the water and liquid salt mixture pool. First a downward zone where the temperature and the heat fluxes along the vessel is rising below a nondimensionnal height in the range 0.6 to 0.75, corresponding to an angle along the vessel of 50 to 76 degrees. Then, above there is an upper zone characterized by a constant temperature and heat fluxes along the vessel, where both the temperature and the heat fluxes reaches their maximum value. For eutectic salt mixture experiments, the variation of the heat generation rate (or Ra' value) does not change the upward and downward Nusselt number (Nu), even if a thicker crust (occurring for a lower heat generation rate) locally imposes a greater thermal resistance. In the non-eutectic cases, a decrease in the heat generation rate is accompanied by a decrease of both the upward and the downward Nusselt number, due to a thicker mushy zone. Note that the upward/downward Nu ratio stays constant during this decrease. For both eutectic and non-eutectic cases, when the cooling water temperature increases, both upward and downward Nusselt numbers increase, however, the ratio between them remains constant. For the salt experiments, downward Nusselt numbers show a good agreement with previous results, whereas upward Nu values are under estimated [37].

Stratified pool test series

A classification in miscible fluids stratification is established, as, stratification with unstable interface for low density difference ($<5\%$) between the two layers, and stratification with stable interfaces for high density difference ($>5\%$). This classification is consistent with other stability criteria present in the literature [32], [36]. Boiling of the lower layer enhances dramatically the upward heat transfer and then increases, at least by a factor 2, the upward/downward splitting of total heat. The upward/downward splitting of total heat

is affected by the stratification, more heat is transferred downwards when stratification is present. Miscibility of the two layers has to be taken into account since immiscibility of the two layers makes more heat to flow downward compared to miscible fluids. The upward heat transport increases when both layers have heat generation. For larger density differences ($>5\%$) between the two layers, the interface is sharper and imposes a greater resistance for the upward heat transport. The mixing time scale is directly dependent on the power supplied in the pool, it increases when the power supply decreases and, also, when both layers have heat generation. The lower layer of a stratified pool is characterized by an increasing temperature and heat flux along the vessel wall until both reach their maximum value just below the interface. In the upper layer, both the temperature and the heat flux decrease from the maximum value at the interface. A mixing process of both layers heated has been observed. First the upper layer mixes with an intermediate layer in the lower layer. Then it creates a new thicker upper layer which mixes with the remaining lower layer. When both layers are heated, and for stable interface, the stratification is a stable configuration since no complete mixing is observed as a steady state is reached slowly.

4.3.2 FOREVER experimental program

The second FOREVER (Failure Of REactor VESsel Retention) integral test - FOREVER-C2 was performed to investigate natural convection heat transfer and reactor pressure vessel creep deformation and failure during the late-stage of in-vessel melt progression under nuclear power plant severe accident conditions.

The distinguishable feature of the FOREVER-C2 test, in comparison to the all previous FOREVER-C1 and LHF-1,...,8 (performed in Sandia NL) tests, is the high-temperature conditions of the vessel ($950-1000^{\circ}\text{C}$ vs. $700-800^{\circ}\text{C}$ external wall temperature in the FOREVER-C1 and $\approx 700^{\circ}\text{C}$ in all LHF tests); and low-pressure-loadings (25 bars vs. 100 bars in the LHF experiments).

The facility employs a 1/10-scaled 15MND5-(FRAMATOME)-steel vessel of 400mm diameter, 15mm wall thickness and 750mm height. A high-temperature ($\approx 1300^{\circ}\text{C}$) oxide melt is prepared in a SiC-crucible placed in a 50kW induction furnace and is, then, poured into the test-vessel. A MoSi_2 60kW electric heater is employed in the melt pool to heat and maintain its temperature at $1200-1300^{\circ}\text{C}$. During the FOREVER-C2 test, the power was kept at the 30-45kW level, in order to achieve external wall maximum temperature in the range of $950-1000^{\circ}\text{C}$. The vessel was pressurized with Argon at the desired pressure (25 bars for the FOREVER-C2 test).

The FOREVER-C2 experiment was performed on June 3, 1999. After the melt delivery and sealing of the vessel, the heater power Q was raised to the range of 30-35kW, Figure 4.13. After approximately two hours of heating, the thermal steady-state was achieved, with maximum external wall temperature $950-1000^{\circ}\text{C}$ and the maximum melt pool temperature in the range of $1200-1300^{\circ}\text{C}$, see Figure 4.14.

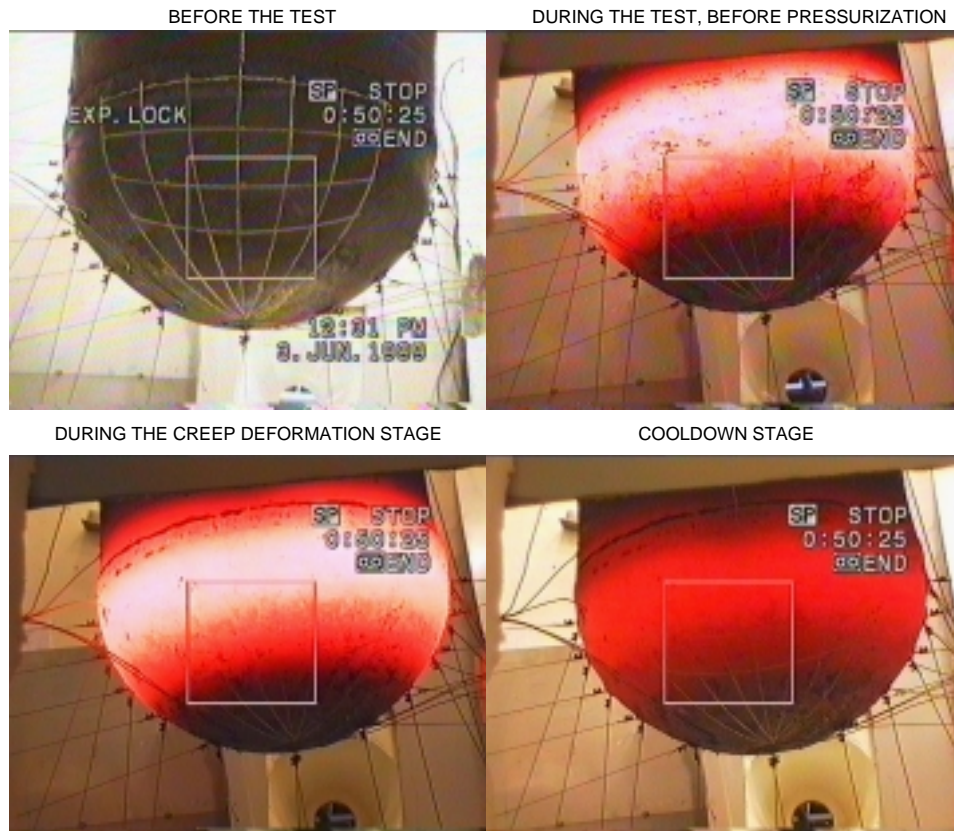


Fig. 4.12: View of the vessel during the test.

After approximately 2 hrs of the test, the power was temporarily shutdown, due to overheating of the cables and the necessity to provide additional cooling for the cables. By the end of the 3rd hour of the test, the steady-state conditions were re-stored, and the pressurization system was activated. The pressure level was raised to 24-25 bars, and kept at this level for nearly three hours, during which the vessel creep deformation was recorded. By the end of the 3rd hour of the pressurization (and the 6th hour of the test), the maximum recorded creep deformation reached 20 mm, which corresponds to approximately 10% of the hoop strain, ε_h , Figure 4.13. Notably, during the creep deformation stage, the creep rate acceleration is observed, with the creep rate of $\dot{\varepsilon}_h \simeq 1\text{mm}/20\text{min}$ at the beginning of the test, and $\dot{\varepsilon}_h \simeq 1\text{mm}/5\text{min}$ near the end of the test. This clearly indicates the 'strain-hardening' nature of the creep law for 15MND5-(FRAMATOME)-steel.

On the 7th hour of the test, the heater failure occurred, and the test was terminated. Post-test examination of the heater revealed that the heater failure could be caused by either a defect at the welded joint or by overheating due to melt pool level drop and uncover of the upper portion of the heater.

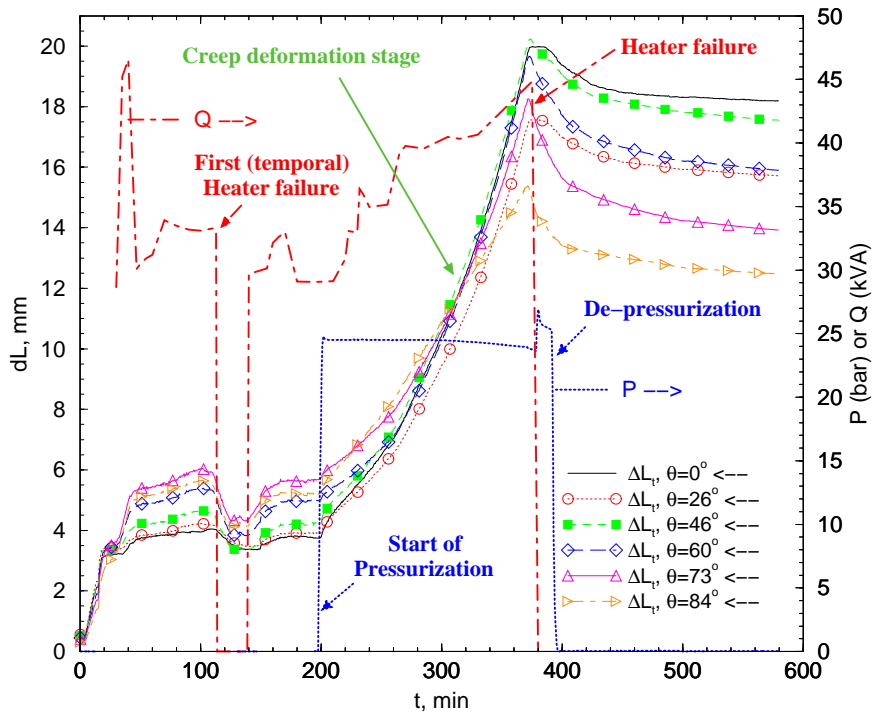


Fig. 4.13: Preliminary data for creep deformation.

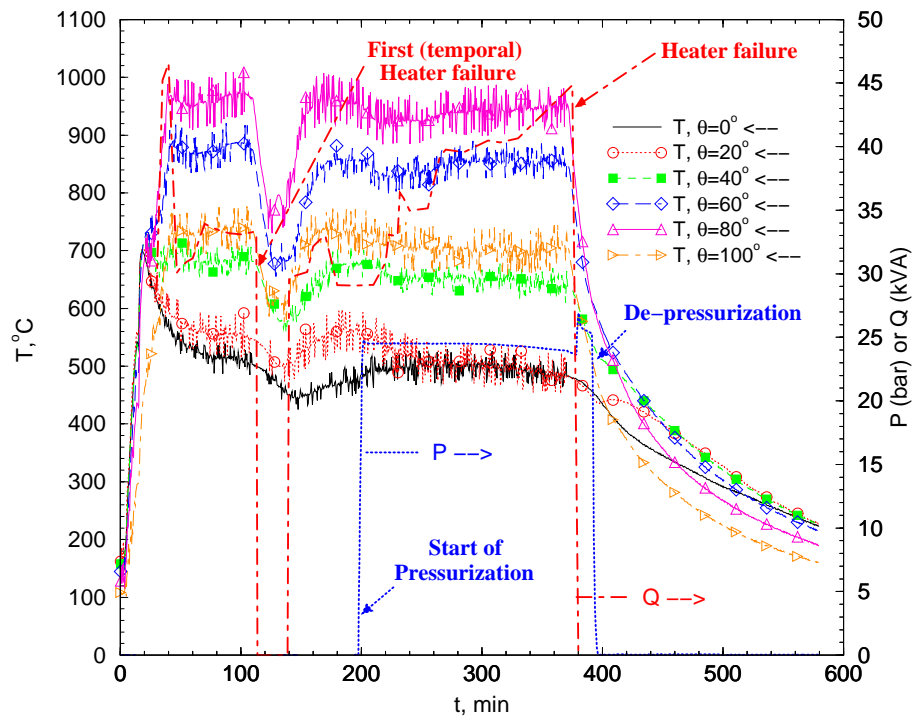


Fig. 4.14: Preliminary data for thermal loading.

Chapter 5

Concluding remarks

We believe that significant technical advances have been achieved during the course of these studies at RIT/NPS. It was found that:

- The coolant temperature has significant influence on the characteristics of debris fragments produced from the jet breakup. At low subcooling the fragments are relatively large and irregular compared to smaller particles produced at high subcooling.
- The melt jet density has considerable effect on the fragment size produced. As the melt density increases the fragment size becomes smaller. The mass mean size of the debris changes proportionally to the square root of the coolant to melt density ratio.
- The melt superheat has little effect on the debris particle size distribution produced during the melt jet fragmentation.
- The impingement velocity of the jet has significant impact on the fragmentation process. At lower jet velocity the melt agglomerates and forms a cake of large size debris. When the jet velocity is increased more complete fragmentation is obtained.
- The scaling methodology developed during 1998 is further validated against almost all of the spreading experimental data available so far.
- Experimental results for the dryout heat flux of homogeneous particulate debris beds with top flooding compare well with the Lipinski correlation. For the stratified particle beds, the fine particle layer resting on the top of another particle layer dominates the dryout processes.
- Experimental results show that a downcomer may enhance the dryout heat flux from 50% to 350%.
- The experimental observations show that the stratification and mixing in the pool have profound effect on the heat flux distribution on the pressure vessel lower head.

- The FOREVER-C2 test provides new unique data for high-temperature multi-axial creep deformation of the prototypical reactor pressure vessel and for natural convection heat transfer in hemispherical melt pool.

These studies will be continued in the research program at RIT/NPS sponsored by the Swedish Nuclear Power Inspectorate (SKI), Swiss Federal Nuclear Inspectorate (HSK), USNRC, the European Union, Swedish and Finnish power companies. An EU Project, named ARVI (Assessment of Reactor Vessel Integrity) will be coordinated by Prof. Sehgal, under which further FOREVER experiments will be performed.

Bibliography

- [1] B.R. Sehgal, T.N. Dinh, T.J. Okkonen, V.A. Bui, R.R. Nourgaliev, and J. Andersson, 1996, Studies on Melt-Water-Structure Interactions During Severe Accidents, Nordic Nuclear Safety Research. Report NKS/RAK-2(96)TR-A2, 131p.
- [2] T. Okkonen, T.N. Dinh, V.A. Bui and B.R. Sehgal, 1995, Quantification of the ev-vessel severe accident risks for the Swedish boiling water reactors, A scoping study performed for the APRI Project. SKI Report 95:76, 194p.
- [3] B.R. Sehgal, T.N. Dinh, R.R. Nourgaliev, 1996, Analysis of natural convection in volumetrically-heated melt pools. SKI Report 97:24, 130p.
- [4] B.R. Sehgal, T.N. Dinh, J.A. Green, D. Paladino, 1997, Experimental investigations on vessel-hole ablation during severe accidents. SKI Report 97:44, 91p.
- [5] B.R. Sehgal, T.N. Dinh, V.A. Bui, J.A. Green, R.R. Nourgaliev, T.O. Okkonen and A.T. Dinh, 1998, Experiments and analyses on melt-structure-water interactions during severe accident, SKI report 98:21, 250p.
- [6] B.R. Sehgal, Z.L. Yang, T.N. Dinh, R.R. Nourgaliev, V.A. Bui, H.O. Haraldsson, H.X. Li, M. Konovakhin, D. Paladino, W.H. Leung, 1999, Investigation on melt-structure-water (MSWI) during severe accidents, SKI Report 99:42, 156p.
- [7] T.G. Theofanous, 1995, The Study of Steam Explosions in Nuclear Systems, Nuclear Engineering and Design, 155, pp.1-26, 1995.
- [8] M.L. Corradini, B.J. Kim and M.D. Oh, 1988, Vapor Explosions in Light Water Reactors: a Review of Theory and Modelling. Progress in Nuclear Energy, Vol. 22, No. 1, pp. 1-117.
- [9] M. Bürger, S. H. Cho, E. v. Berg, A. Schatz, 1995. Breakup of Melt Jet as Preconditions for Premixing. *Nucl. Eng. Des.* **155**, 215-251.
- [10] G. Berthoud, 1995. Progress Made in the Area of Molten Fuel Coolant Interactions Proceeding of FISA 95 Symposium on EU Research on Severe Accidents, Luxemburg, 119-139.

- [11] D. Magallon, et al., 1995. High temperature Melt/Water Mixing: Results and Calculations of FARO, PREMIX and MIXA Experiments. Proceeding of FISA 95 Symposium on EU Research on Severe Accidents, Luxemburg, 140-164.
- [12] B.D. Turland, G.P. Dobson, 1996. Molten Fuel Coolant Interactions: A State of the Art Report. EUR 16874 EN, Luxemburg.
- [13] V.A. Bui, T.N. Dinh, B.R. Sehgal, 1997. Numerical Simulation of Surface Instability Phenomena Associated with Fuel Coolant Interactions. Proceedings of the Eight International Topical Meeting on Nuclear Reactor Thermal Hydraulics (NURETH-8), Kyoto, Japan.
- [14] T.N. Dinh, V.A. Bui, R.R. Nourgaliev, J.A. Green, B.R. Sehgal, 1999. Experimental and Analytical Studies of Melt Jet-Coolant Interactions: A Synthesis. *Nucl. Eng. Des.* , in press.
- [15] H.O. Haraldsson, H.X. Li, T.N. Dinh, J.A. Green, B.R. Sehgal, 1997. Hydrodynamic Fragmentation of Molten Metal Jet in Water: Effect of Melt Solidification and Coolant Voiding. Twelfth Proceedings of Nuclear Thermal Hydraulics, 1997 ANS Winter Meeting, Albuquerque, New Mexico.
- [16] R.R. Nourgaliev, T.N. Dinh, B.R. Sehgal, 1997. Simulation of Multiphase Mixing by a Particle Transport Model 5th International Conference on Nuclear Engineering, Nice, France.
- [17] B.R. Sehgal and B.W. Spencer, 1992, ACE Program Phase D: Melt Attack and Coolability Experiments (MACE) Program. Proceedings of the Second OECD(NEA)CSNI Specialist Meeting on Molten Core Debris-Concrete Interactions, Karlsruhe, Germany, April 1-3, KfK 5108. NEA/CSNI/R(92)10.
- [18] H. Alsmeyer, B.Spencer and W. Tromm, 1998, The COMET-Concept for Cooling of Ex-Vessel Corium Melts, ICONE-6, May 10-15, San Diego.
- [19] M. Becker, J. Engstrom and R.V. Macbeth, 1990, Enhancement of Core Debris Coolability, RIT-Report: KTH-NEL-51.
- [20] G.L. Thinnis, 1988, TMI-2 Lower Head Creep Rupture Analysis, *EGG-TMI-8133*, August.
- [21] V. Shah, 1986, Creep Rupture Failure of Reactor Pressure Vessel Lower Head During Severe Accidents, *International ANS/ENS Topical Meeting on Operability of Nuclear Power Systems in Normal and Adverse Environments*, Albuquerque, NM, September 29.
- [22] B.R. Sehgal, R.R. Nourgaliev, T.N. Dinh, 1999, Characterization of heat transfer processes in a melt pool convection and vessel-creep experiment, CD-ROM Proceedings of NURETH-9, San Francisco, Oct. 3-8.
- [23] T.Y. Chu, M.M. Pilch, and J.H. Bentz, 1997, An Assessment of the Effects of Heat Flux Distribution and Penetration on the Creep Rupture of a Reactor Vessel Lower Head, *Twelfth Proceedings of Nuclear Thermal Hydraulics*, 1997 ANS Winter Meeting, November 16-20, Albuquerque, NM, 135-144.

- [24] B.R. Sehgal, R.R. Nourgaliev, T.N. Dinh, V.A. Bui, J.A. Green, and A. Karbojian, 1998, FOREVER Experiment on Thermal and Mechanical Behavior of a Reactor Vessel during a Severe Accident, *Proceedings of the OECD/CSNI Workshop on 'In-Vessel Core Debris Retention and Coolability'*, Garching, Germany, 3-6 March.
- [25] B.R. Sehgal, R.R. Nourgaliev, T.N. Dinh, and A. Karbojian, 1998, Integral Experiments on In-Vessel Coolability and Vessel Creep: Results and Analysis of the FOREVER-C1 test, *Proceedings of the SARJ-98, Workshop on Severe Accident Research held in Japan*, Tokyo, Japan, 4-6 November.
- [26] B.R. Sehgal, R.R. Nourgaliev, T.N. Dinh, and A. Karbojian, 1999, FOREVER Experimental Program on Reactor Pressure Vessel Creep Behavior and Core Debris Retention, *Proceedings of the SMiRT-15, 15th International Conference on Structural Mechanics in Reactor Technology*, Seoul, Korea, 15-20 August.
- [27] V.V. Asmolov., 1998, Latest Findings of RASPLAV Project, OECD/CSNI Workshop on In-Vessel Core Debris Retention and Coolability.
- [28] T.N. Dinh, M. Konovalikhin, D. Paladino, J.A. Green, A.A. Gubaidulin, and B.R. Sehgal, 1998, Experimental Simulation of Core Melt Spreading on a LWR Containment Floor in a Severe Accident, CD-ROM Proceedings International Conference on Nuclear Engineering, ICONE-6, San Diego, CA, USA, May.
- [29] M.J. Konovalikhin, T.N. Dinh and B.R. Sehgal, 1999, The scaling model of core melt spreading: validation, refinement and reactor application. OECD Workshop on Ex-vessel Debris Coolability, Karlsruhe, Germany, 16-18 November
- [30] V.A. Bui, R.R. Nourgaliev, Z.L. Yang, T.N. Dinh, and B.R. Sehgal, 1998, Advances in MVITA Modeling of Thermal Processes in the Reactor Pressure Vessel Lower Plenum with a Core Melt Pool, CD-ROM Proceedings of International Conference on Nuclear Engineering, ICONE-6, San Diego, CA, USA, May.
- [31] D. Paladino, A.S. Theerthan and B.R. Sehgal, 1999, Experimental investigation of debris coolability by bottom injection, ANS 1999 annual meeting and embedded topical meeting, Boston, Massachusetts, June 6-10.
- [32] F.M. Richter and D.P. McKenzie. 1981, On some consequences and possible causes of layered Mantle convection. *J. Geophysical Research*, 86, No B7, pp 6133-6142.
- [33] B.R. Sehgal, T.N. Dinh, J.A. Green, M. Konovalikhin, D. Paladino, W.H. Leung, A.A. Gubaidullin, 1997, Experimental investigation of melt spreading in one-dimensional channel, RIT/NPS Research Report for European Union EU-CSC-1D1-97, 86p.
- [34] B.R. Sehgal, T.N. Dinh, M. Konovalikhin, D. Paladino, A.A. Gubaidullin, 1998, Experimental investigation on melt spreading in one and two dimensions, RIT/NPS Report EU-CSC-2D1-98, December.
- [35] B.R. Sehgal, Z.L. Yang, T.N. Dinh, and D. Paladino, 1998, Investigation of ex-vessel debris coolability by bottom coolant injection, CD-ROM Proceedings International Conference on Nuclear Engineering, ICONE-6, San Diego, CA, USA, May.

- [36] J.S. Turner. 1965, The coupled turbulent transport of salt and heat across a sharp density interface. Intl. J. Heat Mass Transfer, 23, pp. 759-767.
- [37] T.G. Theofanous et.al., 1994, In-Vessel Coolability and Retention of a Core Melt”, DOE/ID-10460.
- [38] B.R. Sehgal et al., 1997, Core Melt - Pressure Vessel Interactions During a LWR Severe Accident (MVI)”, FISA-97 Symposium on EU Research on Severe Accidents, November 17-19, Luxembourg.